River flow mass exponents with fractal channel networks and rainfall

Brent M. Troutman [a,*], Thomas M. Over [b,1]

[a] *US Geological Survey, Denver Federal Center, Box 25046, Mail Stop 413, Lakewood, CO 80225, USA*
[b] *Department of Civil Engineering, Texas A&M University, College Station, TX 77843, USA*

Abstract

An important problem in hydrologic science is understanding how river flow is influenced by rainfall properties and drainage basin characteristics. In this paper we consider one approach, the use of mass exponents, in examining the relation of river flow to rainfall and the channel network, which provides the primary conduit for transport of water to the outlet in a large basin. Mass exponents, which characterize the power-law behavior of moments as a function of scale, are ideally suited for defining scaling behavior of processes that exhibit a high degree of variability or intermittency. The main result in this paper is an expression relating the mass exponent of flow resulting from an instantaneous burst of rainfall to the mass exponents of spatial rainfall and that of the network width function. Spatial rainfall is modeled as a random multiplicative cascade and the channel network as a recursive replacement tree; these fractal models reproduce certain types of self-similar behavior seen in actual rainfall and networks. It is shown that under these modeling assumptions the scaling behavior of flow mirrors that of rainfall if rainfall is highly variable in space, and on the other hand flow mirrors the structure of the network if rainfall is not so highly variable. © 2001 Elsevier Science Ltd. All rights reserved.

Keywords: Rainfall–runoff relationship; Rainfall; Streamflow; Channel networks; Scaling exponent; Multiscaling; Recursive replacement tree; Random multiplicative cascade; Network width function

1. Introduction

A classic problem in hydrologic science is prediction of river flow properties given the knowledge of rainfall and drainage basin properties. Although many approaches have been used for flow prediction, recent significant advances have been made using the framework of scaling invariance. It is by now well known that both river networks, representing the primary mechanism for transport of water over the surface of large basins, and rainfall exhibit certain forms of scaling invariance (see, e.g., [1,11,18,24,29,32,36,41,46,52]). Given that both rainfall and the network obey certain scaling laws, an important ongoing research problem is to understand what type of structure this induces on the resulting flow through the network, both spatially and in time. A significant step in addressing this problem was made by Gupta et al. [20], where the scaling structure of rainfall was modeled using a multifractal description (in particular, a random cascade), and that of networks using a self-similar Peano tree. In this paper we consider a similar scenario, but use a more general recursive replacement model for networks. We shall describe the properties of the network, rainfall, and the resulting flow by *mass exponents*, which characterize the power-law behavior of moments as a function of scale. Mass exponents are particularly useful for examining scaling properties of processes that exhibit a high degree of variability, intermittency, or singularity. They are used as one primary means of characterizing multifractal behavior [13, Chapter 6]. Our main result in this paper (Theorem 3) is an expression relating rainfall, network, and flow mass exponents. This expression reveals that in some cases flow reflects the network scaling, and in other cases flow reflects the rainfall scaling. The main factor determining which of the two constituent processes dominates in flow scaling is degree of spatial variability of rainfall.

---

* Corresponding author. Tel.: +1-303-236-5038; fax: +1-303-236-5034.

E-mail addresses: troutman@usgs.gov (B.M. Troutman), tmover@hotmail.com (T.M. Over).

[1] Currently at University of Illinois at Urbana-Champaign and Eastern Illinois University.

In this paper we are interested in particular in characterizing the time structure of flow at a single point, the outlet of a drainage basin, given an instantaneous burst of (spatially varying) rainfall over the basin. Flow response resulting from such a burst of rainfall has been widely studied by hydrologists and is known as the "instantaneous unit hydrograph" of the basin. Thus, the flow mass exponent that we study is defined in terms of the temporal distribution of flow at the outlet, whereas the rainfall mass exponent is defined in terms of spatial distribution of rainfall over the basin. The channel network (through an assumption of spatially uniform flow velocity) provides the mechanism of relating one to the other, so it is the space-to-time transformation defined by the geometry of the network that we are interested in examining. This approach is in contrast to, for example, that taken in other studies which consider how the *temporal* distribution of rainfall is related to the temporal distribution of flow (e.g., [42,53]). Understanding the relative effects of temporal and spatial variabilities of rainfall is an important and difficult question in hydrology. These effects clearly are very dependent on the time scale of interest. In order to make the problem more manageable, our framework here is to assume that a rainfall event occurs over a very short time period (hence the designation "instantaneous") resulting in flow which would then reflect only spatial rainfall variability over the basin. For rainfall that is not instantaneous in time, linear theory (convolution) provides one way to obtain the time distribution of flow (e.g., [6, Chapter 7]) from the instantaneous unit hydrograph, although then distinguishing the effects of both sources of rainfall variability becomes much more difficult. This paper thus represents an initial step in a treatment of the full space–time problem. We do, however, indicate in a section near the end of the paper how to generalize by considering flow as a space–time process (although still with instantaneous rainfall). This generalization allows us to make connections with results presented in [20].

To introduce notation, we let Γ denote the set of points constituting a drainage basin. With each point $\gamma \in \Gamma$ associate a flow distance $d(\gamma)$ to the outlet through the network draining the basin. We shall assume that the drainage network is modeled by a deterministic recursive replacement algorithm, and this algorithm determines properties of the distance function d. We shall assume that abstractions, e.g., losses due to infiltration and evaporation, have already been accounted for, and that transport from the point of deposition is at a constant velocity, so that the time for water deposited at a particular point in Γ to reach the outlet is proportional to network distance of this point from the outlet. Thus without loss of generality we set the velocity to 1 and use distance as a surrogate for time. Finally, we take to μ be a random rainfall measure on Γ representing the pattern of spatially varying rainfall that is instantaneously deposited over the basin; for a subset, $G \subset \Gamma$, $\mu(G)$ is the random mass of water deposited in G. The measure π, flow at the outlet, is given by

$$\pi(D) = \mu(d^{-1}D), \tag{1}$$

where D is an interval representing a set of flow distances, or we may write $\pi = \mu d^{-1}$. Eq. (1) simply states that flow corresponding to a set of distances is the total rainfall over all basin points residing at these distances from the outlet.

Flow distances have been mapped into an interval in the non-negative real line, and in a similar manner we would like to be able to associate the original sequences $\gamma \in \Gamma$ with points in a finite region of R^2. That is, we would like to be able to define the "spatial embedding" of the self-similar tree. There are a number of reasons as to why this embedding is important. First, understanding the connection of spatial rainfall patterns to network geometry depends on this embedding. Secondly, transport mechanisms differ between hillslope and channel, but to build this distinction into a mathematical model clearly would depend on knowing how the network is embedded. The problem of spatially embedding recursive replacement trees, however, is a difficult one, and some progress has been made along these lines [61], but at this point it is not possible to address it with the approach we are taking. Thus, the results we present simply take points in the basin Γ to be indexed by infinite paths in the recursive replacement tree (i.e., the basin is the "boundary" of the tree) and it is assumed that input (rainfall) varies randomly over this boundary, but the spatial embedding is left undefined. We do remark that there are network models which explicitly incorporate the spatial embedding (e.g., [31,45,58,59]), but it is in general not feasible to obtain analytical results for these models as we are able to do here for recursive replacement trees.

The flow measure when rainfall is spatially uniform has special significance. If rainfall is deposited uniformly at the nodes of a finite rooted tree, it is seen that the flow measure simply counts the number of nodes at different distances from the root of the tree. Such a measure is known as the *width function* of the tree. It has been widely used in hydrologic contexts to approximate the instantaneous unit hydrograph [17,23,46,57], and it has been studied in graph theoretic contexts to describe the so-called "height profile" of trees (e.g., [14]).

Let us introduce the definition of mass exponents at this point. For $\varepsilon > 0$, let B_i be the cubes of a ε-mesh that intersect the support of π. The mass exponents corresponding to flow π are then defined to be $\tau(h)$ satisfying

$$\sum_i \pi^h(B_i) \sim \varepsilon^{-\tau(h)} \quad \text{as } \varepsilon \to 0. \tag{2}$$

We may similarly define mass exponents describing the spatial rainfall process and the network width function. A complication arises because of the randomness of rainfall: we must be concerned about mode of convergence in (2) and conditions under which the limit exists. In the theorem giving our main results, we distinguish between $\tau(h)$ as defined in (2) and a corresponding quantity $\chi(h)$ defined using ensemble averages (see, e.g., [21,33]). A major concern in data analysis is how well scaling exponents obtained using the moments in (2) with finite resolution data estimate the theoretical limits defined as $\varepsilon \to 0$. An illustration of the sampling error that may arise from use of finite resolution data is given in the simulation study in Example 3. Recent advances in this direction are given by Troutman and Vecchia [60] and Ossiander and Waymire [38].

2. Fractal channel networks

2.1. Definitions and basic notions

Drainage basins are modeled here by recursive replacement trees, which are a special case of iterated function systems as discussed by Barnsley [2], and have received much attention recently as a model which reproduces self-similar branching behavior seen in actual river networks [8,35,43,54,55,61,62]. Although there are a number of alternative models for channel networks (e.g., [7,31,45,51,58,59]), recursive replacement trees offer certain advantages, including analytical tractability and the fact that ratios based on a Horton–Strahler ordering scheme, which is a widely applicable method for characterizing scaling properties of branching structures (see, e.g., [46]), may be computed exactly for certain classes of these trees. Also, although the recursive replacement tree model we consider in this paper is deterministic, stochastic versions have been developed [9,62].

In modeling channel networks, a distinction has usually been made between "interior" and "exterior" edges in the drainage tree, as these tend to have different geometric and physical properties in actual basins (e.g., [50]). We therefore in what follows use the recursive replacement algorithm as developed by Veitzer [61] which maintains this distinction. Drainage basins will be taken to be modeled as rooted tree graphs, where the root is the basin *outlet*, and we follow the customary usage of referring to the leaves of the tree (nodes of degree 1, excluding the root) as *sources*, and nodes on the unique path from a given node to the root are said to be downstream from the given node. With one exception as noted below, exterior edges are those adjacent to sources, and interior edges are those not adjacent to sources. We begin by defining two rooted labeled trees the *interior generator* and the *exterior generator*, which will be used to replace interior and exterior edges in the recursive tree generation process. Let the nodes in the interior generator be labeled, with v_{I0} taken to be the root, and assume further that there is a second distinguished node (distinct from the root) which is assigned the label v_{I1}. (See the examples below.) Denote by c the distance (i.e., number of edges) between the two nodes v_{I0} and v_{I1}, and we shall assume throughout that $c \geqslant 2$. Similarly, the points in the exterior generator are labeled with root v_{E0} (there is no need for a second distinguished point as with the interior generator). The edges of these generators are labeled exterior if adjacent to a source; the one exception is that the edge adjacent to and downstream from v_{I1} in the interior generator is taken to be interior regardless of whether v_{I1} is a source. We then define the sequence of recursive replacement trees as follows. We begin with the rooted labeled tree t_0 consisting of two nodes connected by an edge which is taken to be either interior or exterior. The sequence of trees obtained by the recursive replacement process will be conditioned on this initial designation. For $n \geqslant 0$, let tree t_n be given, with each edge being either interior or exterior. Each interior edge in t_n is replaced by the interior generator after identifying the downstream node with v_{I0} and the upstream node with v_{I1}. Similarly, each exterior edge is replaced by the exterior generator, with the downstream node being identified with v_{E0}. Tree t_{n+1} is tree t_n with all edges so replaced, and the designation of edges in t_{n+1} as either interior or exterior is identical to the designation in the corresponding replacement generators. We shall refer to the interior or exterior designation of an edge as the edge "type."

Let $n(\alpha', \alpha)$, $\alpha', \alpha \in \{I, E\}$, where I stands for interior and E stands for exterior, be the number of type α edges in the type α' generator, and we can label the edges in the generators with an index taking values in the set $\{1, 2, \ldots, n(\alpha', \alpha)\}$. We shall take α_0 to be the type designation given to the initial edge in tree t_0. Edges in the nth generation tree t_n may be labeled with a length $2n$ sequence of elements $(\alpha_1, v_1; \ldots; \alpha_n, v_n)$, with the $\alpha_i \in \{I, E\}$ designating the sequence of edge types in the recursive replacement process, and with $v_i \in \{1, 2, \ldots, n(\alpha_{i-1}, \alpha_i)\}$, $i \geqslant 1$, identifying edges. Once again, we denote the drainage basin by Γ. We may index the set of points in the drainage basin by Γ the set of infinite paths $\gamma = (\gamma_1, \gamma_2, \ldots)$ where $\gamma_i = (\alpha_i, v_i)$. Equivalently the set Γ may be identified with the "boundary" of the infinite tree obtained by the recursive replacement process. The set of paths in the drainage basin Γ depends on the initial generator α_0, but for purposes of simplifying notation we shall not show this dependence explicitly. We shall denote the curtailment of the infinite sequence γ (i.e., the edges in t_n) by $(\gamma | n) = (\gamma_1, \ldots, \gamma_n)$, and we shall denote the subset of Γ for which the first n elements of the path γ are fixed and equal to $(\gamma | n)$ by $\Gamma_{\gamma | n}$.

Define $f(v; \alpha', \alpha)$ to be the distance of the downstream node of generator edge v from the generator root (i.e., the number of nodes in the unique path to the root), where the generator is type α' and the edge is type α. In tree t_n, the distance of edge $(\gamma | n)$ from the outlet is given by

$$d_{n,\alpha_0}(\gamma | n) = \sum_{i=1}^{n} c^{n-i} f(v_i; \alpha_{i-1}, \alpha_i), \tag{3}$$

where again c is the distance in the interior generator from v_{I0} to v_{I1}. This follows directly from the difference equation

$$d_{n,\alpha_0}(\gamma | n) = c d_{n-1,\alpha_0}(\gamma | n - 1) + f(v_n; \alpha_{n-1}, \alpha_n). \tag{4}$$

The form of (3) suggests that a logical way to define distance to the outlet for the infinite tree Γ is

$$d_{\alpha_0}(\gamma) = \lim_{n \to \infty} \frac{d_{n,\alpha_0}(\gamma | n)}{c^n} = \sum_{i=1}^{\infty} c^{-i} f(v_i; \alpha_{i-1}, \alpha_i). \tag{5}$$

Take $\Delta = [0, \infty)$, the non-negative real numbers. The subset of Δ representing possible flow distances, i.e., $d_{\alpha_0}(\Gamma)$, can be represented as a finite interval $[0, \sigma_{\alpha_0}]$ in the real line. The upper limit σ_{α_0} is defined by $\sigma_{\alpha_0} = \sup\{d_{\alpha_0}(\gamma) : \gamma \in \Gamma\}$. It is seen from (4) and (5) that σ_{α_0} may be found by solving

$$\sigma_{\alpha_0} = \frac{1}{c} \max_{\alpha} [\bar{f}(\alpha_0, \alpha) + \sigma_\alpha],$$

where $\bar{f}(\alpha_0, \alpha) = \max_v f(v; \alpha_0, \alpha)$.

We use a similar notational convention for denoting subsets of $\Delta = [0, \infty)$ as we used for denoting subsets of Γ. The form of the distance function in Eq. (5) suggests that we use a base-c representation of flow distances. Because the $f(v_i; \alpha_{i-1}, \alpha_i)$ may be greater than $c - 1$, flow distances may be greater than 1. We shall find it convenient to follow the convention of representing only the *fractional part* of flow distances in base c form but represent the whole part as any non-negative integer. Thus, consider a sequence of non-negative integers $\delta = \{\delta_0, \delta_1, \ldots\}$, with all except δ_0 obeying the constraint $\delta_i \in \{0, 1, \ldots, c - 1\}$, $i \geq 1$. For given curtailment $\delta | m = \delta_0, \delta_1, \delta_2, \ldots, \delta_m$ we define $\Delta_{\delta | m}$ to be the subset of Δ for which the first $m + 1$ elements in the path δ are $\delta_0, \delta_1, \delta_2, \ldots \delta_m$. That is, $\Delta_{\delta | m}$ is the interval

$$\Delta_{\delta | m} = \left[\sum_{i=0}^{m} c^{-i} \delta_i, \sum_{i=0}^{m} c^{-i} \delta_i + c^{-m} \right).$$

It is seen that in representing flow distances the first coefficient will obey $\delta_0 \in \{0, 1, \ldots, c^* - 1\}$, where c^* is 1 plus the greatest integer *less than* $\max(\sigma_{\alpha_0})$.

2.2. The width function

For fixed distance j, the *width* of the rooted tree t_n is the number of edges with downstream node at distance j from the root. Considered as a function of j, the width function is proportional to the probability mass function of distance from the root of a randomly chosen edge. Define

$$N_{n,\alpha_0}(x) = \# \left\{ (\gamma | n) : \frac{d_{n,\alpha_0}(\gamma | n)}{c^n} < x \right\},$$

representing the *cumulative* width function for tree t_n. We shall look at the asymptotic behavior of this as n grows large in order to characterize the width function for the basin Γ. The properties of $N_{n,\alpha_0}(x)$ may be related to the interior and exterior generator width functions. Let $n_j(\alpha_0, \alpha)$ be the number of type α edges in the type α_0 generator at distance j from the root. From (4), $N_{n,\alpha_0}(x)$ obeys the difference equation

$$N_{n,\alpha_0}(x) = \sum_{\alpha} \sum_{j} n_j(\alpha_0, \alpha) N_{n-1,\alpha}(cx - j). \tag{6}$$

Next let

$$N_{n,\alpha_0} = \lim_{x \to \infty} N_{n,\alpha_0}(x)$$

be the *total* number of nodes in tree t_n with initial edge type α_0. It is seen from (6) that N_{n,α_0} obeys

$$N_{n,\alpha_0} = \sum_{\alpha} n(\alpha_0, \alpha) N_{n-1,\alpha}. \tag{7}$$

Let b (b') denote the maximum (minimum) eigenvalue of the 2×2 matrix $\{n(\alpha', \alpha)\}$,

$$b, b' = \frac{n(I,I) + n(E,E) \pm \sqrt{[n(I,I) - n(E,E)]^2 + 4n(I,E)n(E,I)}}{2}. \tag{8}$$

Then from (7) it follows that asymptotically

$$N_{n,\alpha_0} \sim C(\alpha_0) b^n, \quad n \to \infty, \tag{9}$$

where, using the initial condition $N_{0,\alpha_0} = 1$ (one initial edge), the constants $\{C(\alpha_0)\}$ are given by

$$C(\alpha_0) = \frac{\sum_\alpha n(\alpha_0, \alpha) - b'}{b - b'}.$$

Define a probability measure ρ_{α_0} on (Borel) subsets of the real line corresponding to the limiting width function by

$$\rho_{\alpha_0}[0, x] = \lim_{n \to \infty} \frac{N_{n,\alpha_0}(x)}{N_{n,\alpha_0}}.$$

This is simply the limiting probability that a randomly chosen edge will lie at distance less than x from the outlet. Using (6) and (9) it then follows that

$$\rho_{\alpha_0}[0, x] = \sum_\alpha \phi(\alpha_0, \alpha) \sum_j n_j(\alpha_0, \alpha) \rho_\alpha[0, cx - j], \tag{10}$$

where $\phi(\alpha_0, \alpha)$ is the limiting fraction of points in a tree with initial generator type α_0 that drain into a type α edge of this initial tree and is given by

$$\phi(\alpha_0, \alpha) = \frac{C(\alpha)}{\sum_{\alpha'} n(\alpha_0, \alpha') C(\alpha')} = \frac{C(\alpha)}{bC(\alpha_0)}. \tag{11}$$

Finally, it then may be shown from (10) that

$$\rho_{\alpha_0}(\Delta_{\delta_0, \delta_1, \delta_2, \ldots, \delta_m}) = \sum_\alpha \phi(\alpha_0, \alpha) \sum_{i=0}^{c^*-1} n_{\delta_0 c + \delta_1 - i}(\alpha_0, \alpha) \rho_\alpha(\Delta_{i, \delta_2, \ldots, \delta_m}). \tag{12}$$

From (12) we may obtain properties of the mass exponent for the width function measure. The mass exponent for the network width function will be denoted by $\chi_{\text{net}}(h)$. We use χ rather than τ as in Eq. (2) for reasons which will become apparent in the following section on modeling rainfall. Thus, it is desired to find the exponent $\chi_{\text{net}}(h)$ such that

$$\frac{\log \sum_{\delta \mid m} \rho_{\alpha_0}^h(\Delta_{\delta \mid m})}{m \log c} \to \chi_{\text{net}}(h), \quad m \to \infty.$$

Define the matrix $A(h)$, for positive integers h, by

$$A(h) = \left(\sum_{\delta_1} \prod_{i=1}^{h} n_{\delta_0(i)c + \delta_1 - \delta_0'(i)}(\alpha_0(i), \alpha_0'(i)) \right),$$

where the rows in $A(h)$ are indexed by $\delta_0(1), \alpha_0(1); \delta_0(2), \alpha_0(2); \ldots; \delta_0(h), \alpha_0(h)$ and the columns by these indices primed. Each δ_0 may take on c^* values and each α_0 may take on 2 values (I or E), making $A(h)$ a $(2c^*)^h \times (2c^*)^h$ matrix. (See examples below.) The following theorem, proven in Appendix A, gives the mass exponent for the width function measure. Note that the mass exponent does not depend on the initial generator for the channel network.

Theorem 1 (Channel network mass exponent). *The mass exponent for the width function of the recursive replacement channel network is given, for positive integers h, by*

$$\chi_{\text{net}}(h) = \frac{\log \omega(h) - h \log b}{\log c},$$

where $\omega(h)$ is the maximum eigenvalue of $A(h)$.

One important question is whether the width function as described by this mass exponent in this theorem exhibits multifractal behavior. Multifractality of the width function is usually defined in terms of nonlinearity of $\chi_{\text{net}}(h)$ in h. The examples presented next will illustrate that the width function for recursive replacement trees may exhibit multifractal behavior (Example 1), but not necessarily so (Example 2). This is a point that is discussed in greater detail for recursive replacement trees by Veitzer [61]. Multifractal modeling of the width function of actual networks was considered by Marani et al. [28], although they applied a random cascade formalism (similar to the model we use for

rainfall below) to investigate the origin of the multifractal behavior rather than a recursive replacement network structure. Veneziano et al. [63] pointed out that there are difficulties in the detection of multifractality when analyzing actual network data. In particular, certain algorithms may spuriously indicate multifractality when none exists. The iterated pulses model discussed by Veneziano et al. [64] yields width functions that are too smooth to exhibit multifractal behavior, although increments of the width function are under certain conditions multifractal. We emphasize at this point that Theorem 3 presented below, which gives an expression for flow mass exponents, holds whether the network width function is multifractal or not.

2.3. Examples

We illustrate these definitions and Theorem 1 with two examples, *regular* networks and the *average Shreve* network, both discussed in detail by Veitzer [61].

2.3.1. Example 1. Regular channel networks

An important special case of recursive replacement trees is when (1) the exterior generator is identical to the interior generator (if the labeling of the node v_{11} is ignored) and (2) c is the maximal distance of nodes to the root in both the generators. (Veitzer [61] refers to this as the *zero overlap* case.) We shall refer to such channel networks as "regular" networks. We fix the initial edge $\alpha_0 = E$ and drop the subscript on d and ρ. Because there is no longer a distinction between interior and exterior generators, we may write $f(v_i; \alpha_{i-1}, \alpha_i)$ as simply $f(\gamma_i)$, and it is seen that $c - 1 = \max_{\gamma_i} f(\gamma_i)$. It follows from (5) that the set of flow distances $d(\Gamma)$ is simply the interval $[0, 1]$, or equivalently, the set of all c-ary trees. Also, for this case $c^* = 1$ and $\delta_0 = 0$, so we may take $\delta \,|\, m = \delta_1, \delta_2, \ldots, \delta_m$. The generator width function (for both interior and exterior generators) is denoted by

$$\tilde{n}_j = \sum_\alpha n_j(\alpha_0, \alpha), \quad j \in \{0, 1, \ldots, c-1\}.$$

Eq. (12) for the width function measure simplifies to

$$\rho(\Delta_{\delta \,|\, m}) = \frac{\tilde{n}_{\delta_1}}{b} \rho(\Delta_{\delta_2 \ldots \delta_m}), \quad m = 2, 3, \ldots,$$

which together with $\rho(\Delta_{\delta_m}) = \tilde{n}_{\delta_m}/b$ leads to the solution

$$\rho(\Delta_{\delta \,|\, m}) = \prod_{k=1}^m \frac{\tilde{n}_{\delta_k}}{b}. \tag{13}$$

Also $\omega(h) = \sum_{i=0}^{c-1} \tilde{n}_i^h$, yielding

$$\chi_{\text{net}}(h) = \frac{\log \sum_{i=0}^{c-1} \tilde{n}_i^h}{\log c} - h \frac{\log b}{\log c} \tag{14}$$

or

$$c^{\chi_{\text{net}}(h)} = \frac{\sum_{i=0}^{c-1} \tilde{n}_i^h}{b^h}.$$

It is also seen from (13) that the width function is equivalent to a multinomial cascade; the result (14) for the mass exponent of the multifractal measures resulting from these cascades is given by Feder [13].

A well-known special case is the Peano basin [15,26,27]. For this network, $b = 4$, $b' = 1$, $c = 2$, $C(I) = C(E) = 1$, $\sigma_I = \sigma_E = 1$, $\tilde{n}_0 = 1$, and $\tilde{n}_1 = 3$. Trees t_0 to t_3 are illustrated in Fig. 1 (with t_1 representing the generator) and the width function is illustrated in Fig. 2. In Fig. 2(a) is plotted $\rho(\Delta_{\delta \,|\, m})/2^{-m}$ versus distance, $\sum_0^m c^{-i} \delta_i$ for $m = 8$. This may be thought of as a "density" at this scale, although in the limit as $m \to \infty$ the density does not exist because the measure ρ is singular. In Fig. 2(b) is shown the cumulative distribution at this same scale. The width function for this tree is equivalent to the measure induced by a binomial multiplicative cascade with fractions 0.25 and 0.75 going into the left and right halves, respectively, of an interval being successively subdivided [13].

2.3.2. Example 2. Average Shreve channel networks

The interior and exterior generators for the "average Shreve" model are shown in Fig. 3; values for $n_j(\alpha_0, \alpha)$ are given in Table 1. This model is known as the average Shreve model because it exhibits certain self-similarity properties
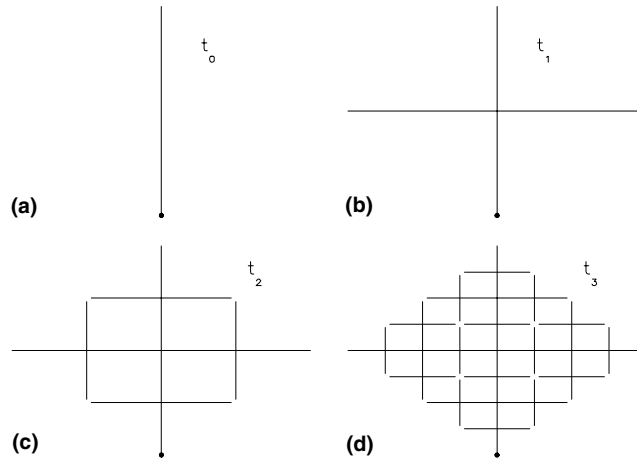
Fig. 1. Trees t_0, t_1, t_2, and t_3 for the Peano recursive replacement network.
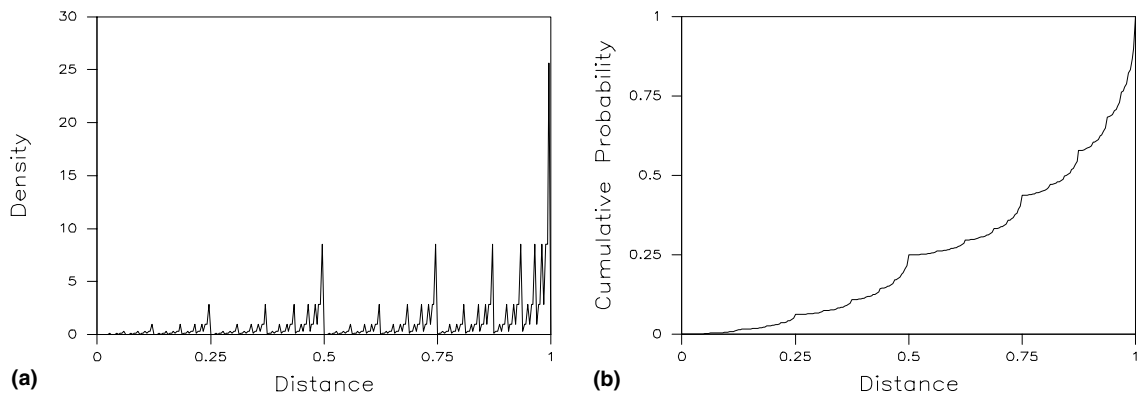

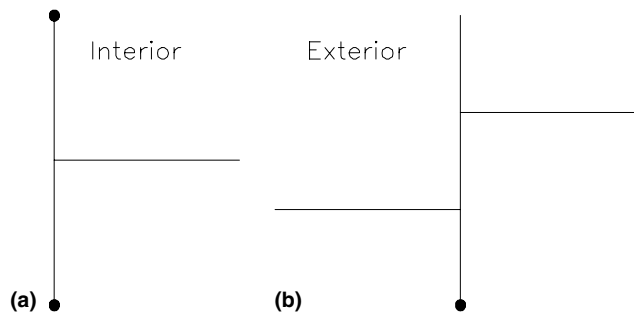Fig. 2. The width function for the Peano recursive replacement network.

Fig. 3. Generators for the average Shreve model.

Table 1
Values of $n_j(\alpha_0, \alpha_1)$ for the average Shreve network

j	α_0, α_1			
	I, I	*I, E*	*E, I*	*E, E*
0	1	0	1	0
1	1	1	1	1
2	0	0	0	2
Sum	2	1	2	3

(see [43,54,55,62]) identical to those of the so-called "random model" in geomorphology [49]. We have for this model $b = 4$, $c = 2$, $C(I) = 2/3$, $C(E) = 4/3$, $\sigma_I = 3/2$, $\sigma_E = 2$, and $c^* = 2$. Trees t_0 to t_3 are illustrated in Fig. 4 (with initial generator E) and Fig. 5 (with initial generator I). The width function is shown in Fig. 6 for both interior and exterior initial generators, again for $m = 8$.

We illustrate construction of the matrix $A(h)$ for $h = 1$ and 2. The elements of the 4×4 matrix $A(1)$ are given in Table 2. All elements are shown, although some elements will be zero because we define $n_j(\alpha_0, \alpha_1) = 0$ for $j < 0$ or $j > 2$. We obtain

$$A(1) = \begin{bmatrix} 2 & 1 & 1 & 0 \\ 0 & 1 & 0 & 1 \\ 2 & 1 & 1 & 0 \\ 0 & 1 & 2 & 3 \end{bmatrix}.$$

Similarly, $A(2)$ is a 16×16 matrix consisting of 4×4 submatrices:

$$\begin{aligned} A(2) &= \{B(\alpha_0(1), \alpha_0(2); \alpha_0'(1), \alpha_0'(2))\} \\ &= \begin{bmatrix} B(I,I;I,I) & B(I,I;I,E) & B(I,I;E,I) & B(I,I;E,E) \\ B(I,E;I,I) & B(I,E;I,E) & B(I,E;E,I) & B(I,E;E,E) \\ B(E,I;I,I) & B(E,I;I,E) & B(E,I;E,I) & B(E,I;E,E) \\ B(E,E;I,I) & B(E,E;I,E) & B(E,E;E,I) & B(E,E;E,E) \end{bmatrix}. \end{aligned}$$

Each of the submatrices has elements shown in Table 3. In this Table, an entry $n_i n_j$ stands for $n_i(\alpha_0(1), \alpha_0'(1)) n_j(\alpha_0(2), \alpha_0'(2))$. The resulting matrix $A(2)$ for the average Shreve model is
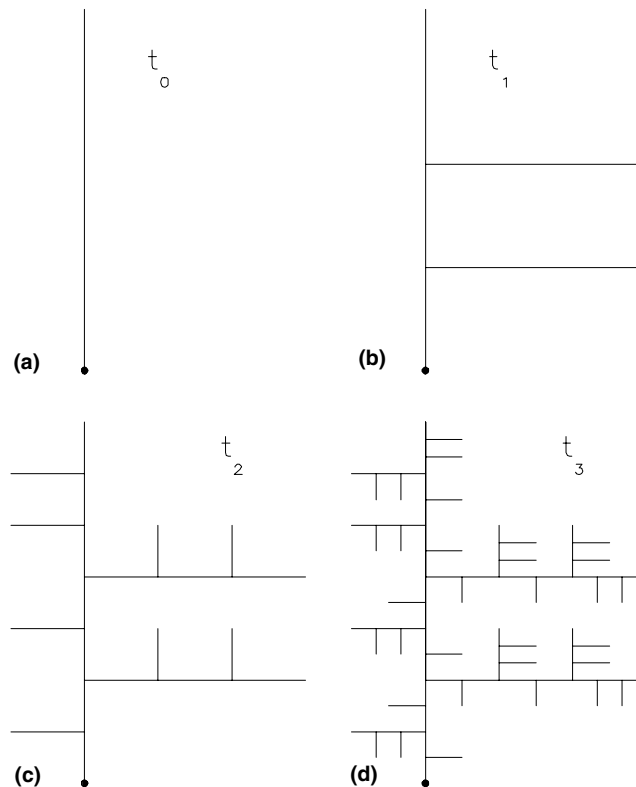

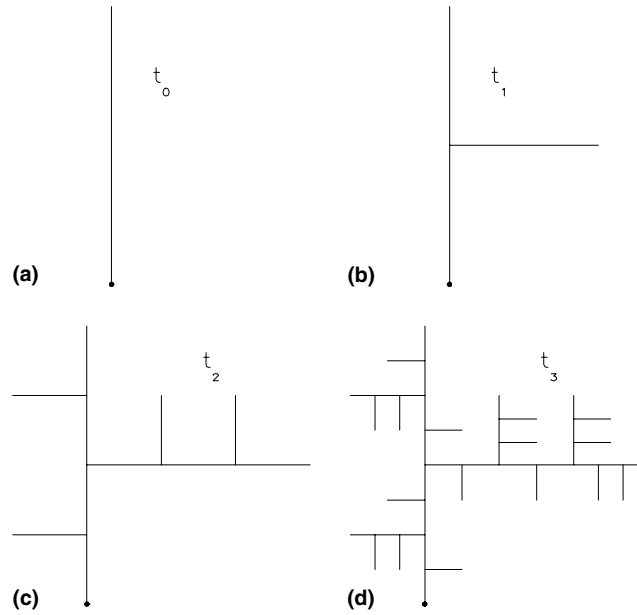Fig. 4. Trees t_0, t_1, t_2, and t_3 for the average Shreve network with exterior initial generator.

Fig. 5. Trees t_0, t_1, t_2, and t_3 for the average Shreve network with interior initial generator.
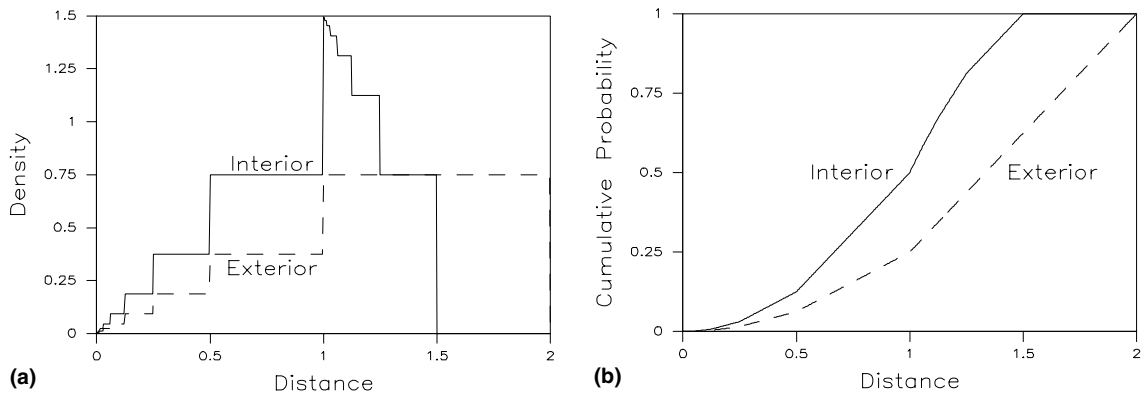

Fig. 6. Width function for the average Shreve model with interior and exterior initial generators.

Table 2
Elements of the matrix $A(1)$ for the average Shreve network

$\alpha_0(1)$, $\delta_0(1)$	$\alpha'_0(1)$, $\delta'_0(1)$			
	I, 0	I, 1	E, 0	E, 1
I, 0	$n_0(I,I) + n_1(I,I)$	$n_{-1}(I,I) + n_0(I,I)$	$n_0(I,E) + n_1(I,E)$	$n_{-1}(I,E) + n_0(I,E)$
I, 1	$n_2(I,I) + n_3(I,I)$	$n_1(I,I) + n_2(I,I)$	$n_2(I,E) + n_3(I,E)$	$n_1(I,E) + n_2(I,E)$
E, 0	$n_0(E,I) + n_1(E,I)$	$n_{-1}(E,I) + n_0(E,I)$	$n_0(E,E) + n_1(E,E)$	$n_{-1}(E,E) + n_0(E,E)$
E, 1	$n_2(E,I) + n_3(E,I)$	$n_1(E,I) + n_2(E,I)$	$n_2(E,E) + n_3(E,E)$	$n_1(E,E) + n_2(E,E)$

Table 3
Elements of the matrix $B(\alpha_0(1), \alpha_0(2); \alpha'_0(1), \alpha'_0(2))$ for the average Shreve network

$\delta_0(1)$, $\delta_0(2)$	$\delta'_0(1)$, $\delta'_0(2)$			
	0, 0	0, 1	1, 0	1, 1
0, 0	$n_0 n_0 + n_1 n_1$	$n_0 n_{-1} + n_1 n_0$	$n_{-1} n_0 + n_0 n_1$	$n_{-1} n_{-1} + n_0 n_0$
0, 1	$n_0 n_2 + n_1 n_3$	$n_0 n_1 + n_1 n_2$	$n_{-1} n_2 + n_0 n_3$	$n_{-1} n_1 + n_0 n_2$
1, 0	$n_2 n_0 + n_3 n_1$	$n_2 n_{-1} + n_3 n_0$	$n_1 n_0 + n_2 n_1$	$n_1 n_{-1} + n_2 n_0$
1, 1	$n_2 n_2 + n_3 n_3$	$n_2 n_1 + n_3 n_2$	$n_1 n_2 + n_2 n_3$	$n_1 n_1 + n_2 n_2$

$$
A(2) = \begin{bmatrix}
2 & 1 & 1 & 1 & 1 & 0 & 1 & 0 & 1 & 1 & 0 & 0 & 1 & 0 & 0 & 0 \\
0 & 1 & 0 & 0 & 0 & 1 & 0 & 0 & 0 & 0 & 0 & 0 & 0 & 0 & 0 & 0 \\
0 & 0 & 1 & 0 & 0 & 0 & 0 & 0 & 0 & 0 & 1 & 0 & 0 & 0 & 0 & 0 \\
0 & 0 & 0 & 1 & 0 & 0 & 0 & 1 & 0 & 0 & 0 & 1 & 0 & 0 & 0 & 1 \\
& & & & & & & & & & & & & & & \\
2 & 1 & 1 & 1 & 1 & 0 & 1 & 0 & 1 & 1 & 0 & 0 & 1 & 0 & 0 & 0 \\
0 & 1 & 0 & 0 & 2 & 3 & 0 & 2 & 0 & 0 & 0 & 0 & 0 & 2 & 0 & 0 \\
0 & 0 & 1 & 0 & 0 & 0 & 0 & 0 & 0 & 0 & 1 & 0 & 0 & 0 & 0 & 0 \\
0 & 0 & 0 & 1 & 0 & 0 & 2 & 1 & 0 & 0 & 0 & 1 & 0 & 0 & 2 & 1 \\
& & & & & & & & & & & & & & & \\
2 & 1 & 1 & 1 & 1 & 0 & 1 & 0 & 1 & 1 & 0 & 0 & 1 & 0 & 0 & 0 \\
0 & 1 & 0 & 0 & 0 & 1 & 0 & 0 & 0 & 0 & 0 & 0 & 0 & 0 & 0 & 0 \\
0 & 0 & 1 & 0 & 0 & 0 & 0 & 0 & 2 & 0 & 3 & 2 & 0 & 0 & 2 & 0 \\
0 & 0 & 0 & 1 & 0 & 0 & 0 & 1 & 0 & 2 & 0 & 1 & 0 & 2 & 0 & 1 \\
& & & & & & & & & & & & & & & \\
2 & 1 & 1 & 1 & 1 & 0 & 1 & 0 & 1 & 1 & 0 & 0 & 1 & 0 & 0 & 0 \\
0 & 1 & 0 & 0 & 2 & 3 & 0 & 2 & 0 & 0 & 0 & 0 & 0 & 2 & 0 & 0 \\
0 & 0 & 1 & 0 & 0 & 0 & 0 & 0 & 2 & 0 & 3 & 2 & 0 & 0 & 2 & 0 \\
0 & 0 & 0 & 1 & 0 & 0 & 2 & 1 & 0 & 2 & 0 & 1 & 4 & 2 & 2 & 5
\end{bmatrix}.
$$

It is easily verified that for this model

$$
\sum_{\delta_0,\alpha_0} n_{\delta_0 c + \delta_1 - \delta_0'}(\alpha_0, \alpha_0') = 2,
$$

independent of δ_1, δ_0' and α_0'. Therefore, the sum of the elements in each column of $A(h)$ is 2^{h+1}, which implies that 2^{h+1} is an eigenvalue of the transpose of $A(h)$ with corresponding eigenvector having all elements equal to unity. It may be shown by induction that if v is any eigenvalue of a matrix B with corresponding eigenvector having all elements equal to 1, then the elements of $v^{-n}B^n$ are bounded (in n), which means that v must be a maximal eigenvalue. Thus, 2^{h+1} is the maximum eigenvalue $\omega(h)$ of $A(h)$, and by Theorem 1 the network mass exponent is

$$
\chi_{\text{net}}(h) = 1 - h.
$$

The mass exponent is linear in h, which indicates the absence of multifractal behavior, a fact that is also shown by Veitzer [61].

3. Fractal rainfall

Given the self-similar drainage basin, we now introduce spatially variable rainfall over the basin using a multifractal model [5,10,18,19,25,32,36,39–41,52]. In this paper we shall take rainfall to be modeled by a multiplicative random cascade. Theory for random cascades has been developed extensively elsewhere (e.g., [21,22,65]) so we shall present only an outline of the framework. We begin with the drainage basin Γ, which may be thought of as the "boundary" of a tree or the set of all infinite paths in the tree. This set is made into a metric space by defining the metric $D(\gamma, \gamma') = \exp(-|\gamma \wedge \gamma'|)$ where $|\gamma \wedge \gamma'|$ denotes the number of edges the two paths γ and γ' have in common. We now consider measures on (Borel) subsets of Γ. Let us first define a measure λ_{α_0} on Γ which will be the rainfall measure on a network with initial generator α_0 when rainfall is spatially uniform. This measure will be defined on subsets $\Gamma_{\gamma|n}$ by

$$
\lambda_{\alpha_0}(\Gamma_{\gamma|n}) = \prod_{i=1}^{n} \phi(\alpha_{i-1}, \alpha_i),
$$

where ϕ is defined in (11). This leads to

$$
\lambda_{\alpha_0}(\Gamma_{\gamma|n}) = \frac{C(\alpha_n)}{b^n C(\alpha_0)}.
$$

Note that the uniform rainfall measure λ_{α_0} is related to the network width function measure ρ_{α_0} by $\rho_{\alpha_0} = \lambda_{\alpha_0} d_{\alpha_0}^{-1}$, analogous to Eq. (1).

Next, to model the spatial variability of rainfall, with each finite sequence $(\gamma|n)$ we associate a non-negative random variable $W_{\gamma|n}$ defined on a probability space $(\Omega, \mathscr{F}, P)$; these random variables constitute the *cascade generator* process. We shall make the assumption throughout that the $\{W_{\gamma|n}\}$ are independent and identically distributed with mean 1. Define

$$P_{n,\alpha_0}(\gamma) = \sum_{\gamma \mid n} W_{\gamma \mid n} I_{\Gamma_{\gamma \mid n}}(\gamma),$$

$$Q_{n,\alpha_0}(\gamma) = P_{1,\alpha_0}(\gamma) P_{2,\alpha_0}(\gamma) \cdots P_{n,\alpha_0}(\gamma),$$

$$\mu_{n,\alpha_0}(B) = Q_{n,\alpha_0} \lambda_{\alpha_0}(B) = \int_B Q_{n,\alpha_0}(\gamma) \lambda_{\alpha_0}(\mathrm{d}\gamma),$$

where B is a (Borel) subset of Γ. Using martingale theory, it may be shown (e.g., [65]) that this sequence of measures converges almost surely to a random measure $\mu_{\alpha_0} = Q_{\infty,\alpha_0} \lambda_{\alpha_0}$. Denote the limiting total mass by $Z_{\infty,\alpha_0} = \mu_{\alpha_0}(\Gamma)$.

For the special case of regular networks (see Example 1), b is simply the branching number or the number of subdivisions made at each successive change in scale. The drainage basin Γ in this special case may be taken to be a b-ary tree. The resulting model is known as a *Mandelbrot cascade*. Properties of the limiting mass Z_{∞,α_0} for this special case were given by Kahane and Peyrière [22]. The model we are considering, with different interior and exterior generators, is somewhat more complicated. The branching number b for the present model is defined in (8) as the maximum eigenvalue of a matrix, and in a sense represents an "average" of interior and exterior branching properties. (The Proof of Theorem 2 in Appendix A reveals why b is defined this way.) Despite this complication, it is straightforward to show that the theory for the Mandelbrot cascade generalizes readily, and that many of the same results carry through. Although we shall not present details, the following results may be demonstrated using methods from random cascade theory as developed in [3,38,65]. First, $EZ_{\infty,\alpha_0} > 0$ if and only if $\chi'_{\mathrm{rain}}(1-) < 0$, where

$$\chi_{\mathrm{rain}}(h) = \log_b EW^h - (h-1) \tag{15}$$

or

$$b^{\chi_{\mathrm{rain}}(h)} = \frac{EW^h}{b^{h-1}}.$$

Also, Z_{∞,α_0} has a finite moment of order $h > 1$ if and only if

$$h < h_c = \sup\{h \geqslant 1 : \chi_{\mathrm{rain}}(h) < 0\}. \tag{16}$$

Note that h_c does not depend on α_0. We shall make the assumption throughout this paper that $\chi'_{\mathrm{rain}}(1-) < 0$.

The quantity of interest is the mass exponent, as defined in Eq. (2). First we define the hth moment

$$M_{n,\alpha_0}(h) = \sum_{\gamma \mid n} \mu_{\alpha_0}^h(\Gamma_{\gamma \mid n}), \tag{17}$$

and when it exists, define the limit

$$\tau_{\mathrm{rain}}(h) = \lim_{n \to \infty} \frac{\log M_{n,\alpha_0}(h)}{n \log b} \tag{18}$$

to be the mass exponent. Because the cascade rainfall is a stochastic model, the moment used in the computation of the mass exponent in (18) is random, so we must be concerned about the mode of convergence and about characterizing the limit in (18). In the following theorem we present a generalization of a result for the Mandelbrot cascade given in [21]; it gives conditions under which the rainfall mass exponent $\tau_{\mathrm{rain}}(h)$ coincides with $\chi_{\mathrm{rain}}(h)$. The proof is similar to that given by Holley and Waymire [21], so details will not be given. One of the key steps, however, is outlined in Appendix A showing how the definition of b in terms of interior and exterior generator properties arises.

Theorem 2 (Rainfall mass exponent). *If $2h < h_c$ and $EW^{2h}/(EW^h)^2 < b$, then with probability 1 the limit in* (18) *exists and is given by*

$$\tau_{\mathrm{rain}}(h) = \chi_{\mathrm{rain}}(h).$$

Thus, $\chi_{\mathrm{rain}}(h)$ may be thought of as an ensemble average mass exponent for the range of values of h in the theorem. We remark that, in the special case of a Mandelbrot cascade, the condition $EW^{2h}/(EW^h)^2 < b$ assumed here is more restrictive than necessary. That is, the conclusion of the theorem may still hold for values of h for which this condition is violated. The theory and approach presented in [21], upon which this result is based, have been generalized, for example, in [33,38,47]. It is known from the more recent work on Mandelbrot cascades that, depending on the behavior of $\chi_{\mathrm{rain}}(h)$, the limit in (18) for h greater than some critical value may not be $\chi_{\mathrm{rain}}(h)$ but rather an exactly linear function of h. It is not known at this point how this theory carries over to the general recursive replacement network model assumed here.

Another point should be made about this cascade model for rainfall. It is apparent that the structure of the rainfall model is tied to the recursive replacement model that is being assumed for networks. This was done mostly for reasons of mathematical tractability in obtaining the results in the following section. Also, because the spatial embedding problem for recursive replacement trees has not been solved, it is unclear how one would generate rainfall over a network without somehow tying the rainfall to the network. There is, however, some reason for believing that the results presented below do not depend in a critical way on this coupling of the models. Even if the Mandelbrot cascade were being used to model rainfall without reference to a channel network, the model depends on selection of branching number (b) which is not uniquely determined by physical considerations. Over [39] and Molchan [34] discuss this problem, and Over [39] shows that use of an infinitely divisible distribution for $\log(W)$ that changes with b may under certain conditions lead to a mass exponent that does not depend on b. In other words, selection of the "correct" value for b would not be a crucial issue in the rainfall modeling process, or, equivalently, fixing b based on external considerations (such as channel network structure) would not have a great influence on the properties of the rainfall model. It is still an open problem what can be said along these lines for the more complicated network structure being modeled in this paper.

4. River flow mass exponents

4.1. Main result

As in Eq. (1), define the flow measure with initial generator α_0 by $\pi_{\alpha_0} = \mu_{\alpha_0} d_{\alpha_0}^{-1}$. Our main results on the flow mass exponent are given in the following theorem, which again is proven in Appendix A.

Theorem 3 (Flow mass exponents). *Let h be a positive integer, $r = \log b / \log c$, and define*

$$\chi_{\text{flow}}(h) = \max[\chi_{\text{net}}(h), r\chi_{\text{rain}}(h)]. \tag{19}$$

(i) *If $h < h_c$ (defined in (16)),*

$$\lim_{m \to \infty} \frac{\log E \sum_{\delta \mid m} \pi_{\alpha_0}^h (\varDelta_{\delta \mid m})}{m \log c} = \chi_{\text{flow}}(h). \tag{20}$$

(ii) *If $2h < h_c$ and $r\chi_{\text{rain}}(2h) < 2\chi_{\text{flow}}(h)$, then with probability 1*

$$\tau_{\text{flow}}(h) := \lim_{m \to \infty} \frac{\log \sum_{\delta \mid m} \pi_{\alpha_0}^h (\varDelta_{\delta \mid m})}{m \log c} = \chi_{\text{flow}}(h). \tag{21}$$

The key element in this theorem is the definition of the flow mass exponent $\chi_{\text{flow}}(h)$ in Eq. (19). It is the maximum of two terms, the network mass exponent and the rainfall mass exponent (scaled by r), indicating that for a given order h, the flow moment scaling will reflect only the more dominant, as measured by magnitude of the mass exponent, of the two constituent processes. Examples of this effect are given below. We remark once again that, as in Theorem 2, it may be possible to relax the conditions in part (ii).

The convergence result in Eq. (21) suggests a straightforward method for estimating the mass exponent based on finite resolution (i.e., measured down to a finite level m) data. In the simulation example that is to be discussed below, a further result is used although we shall not give a detailed derivation here. If the limit in (21) exists, then under certain conditions

$$\frac{\log \sum_{\delta \mid m} \pi_{\alpha_0}^h (\varDelta_{\delta \mid m}) - \log \sum_{\delta \mid m-1} \pi_{\alpha_0}^h (\varDelta_{\delta \mid m-1})}{\log c}, \tag{22}$$

computed using masses at both levels m and $m-1$, converges to the same limit. This quantity may converge more rapidly than (21), thus providing a better estimate of $\chi_{\text{flow}}(h)$. In general more than two levels may be used together with least squares procedures to estimate mass exponents (see, e.g., [39,60]).

4.2. Space–time flow scaling

The results in [20] pertain to scaling of peak flows with drainage area, whereas our results in Theorem 3 are relevant to scaling of "temporal" moments, if we think of distance from the outlet as a surrogate for time. In order to establish the connection of these approaches, let us consider the more general question of flow as a space–time process. The measure π_{α_0} is defined on flow distance to the outlet, which may be thought of as equal to time under the assumption of constant flow velocity of unity throughout the network. The key point is that we are looking at flow at only a single spatial point, the outlet. In general flow in a river basin is a space–time process, and it is of interest to characterize spatial variability of flow properties as well as temporal variability at a given point. The framework we have chosen may be readily extended to look at space–time flow. For given n, let us consider sub-regions $\Gamma_{\gamma|n}$ of Γ, and suppose that we are interested not only in flow at the outlet of Γ but in flow at the outlet of *all* sub-regions $\Gamma_{\gamma|n}$ jointly. We need to revise the definition of the distance function $d_{\alpha_0}(\gamma)$ to account for the fact that we are now looking at flow distances to the sub-region outlets rather than to the outlet of Γ. It will be convenient to look at flow distances in sub-region $\Gamma_{\gamma|n}$ scaled by multiplying by c^n. Accordingly, define $\tilde{d}_{n,\alpha_n}(\gamma)$ to be c^n times distance from γ to the outlet of the sub-region in which γ lies, i.e.,

$$\tilde{d}_{n,\alpha_n}(\gamma) = \sum_{i=1}^{\infty} c^{-i} f(v_{i+n}; \alpha_{i+n-1}, \alpha_{i+n});$$

note that the initial generator for the sub-region is α_n. Using Π_{α_0} to denote the space–time flow measure on $\Gamma \times \Delta$, let $\Pi_{\alpha_0}(\Gamma_{\gamma|n}, \Delta_{\delta|m})$ be the volume of flow at the outlet of sub-region $\Gamma_{\gamma|n}$ resulting from rainfall over $\Gamma_{\gamma|n}$ with scaled flow distance to the sub-region outlet in the set $\Delta_{\delta|m}$. That is,

$$\Pi_{\alpha_0}(\Gamma_{\gamma|n}, \Delta_{\delta|m}) = \mu_{\alpha_0}\left(\Gamma_{\gamma|n} \cap \tilde{d}_{n,\alpha_n}^{-1} \Delta_{\delta|m}\right). \tag{23}$$

Thus, n defines the size, or spatial resolution, of sub-regions of interest and m defines the "temporal" resolution of sub-region flow. Observe that we do not restrict our consideration only to sub-regions which receive no upstream flow from other sub-regions, but instead in defining the flow measure Π_{α_0}, we omit that portion of flow resulting from upstream contributions, so that $\Pi_{\alpha_0}(\Gamma_{\gamma|n}, \Delta) = \mu_{\alpha_0}(\Gamma_{\gamma|n})$ and $\Pi_{\alpha_0}(\Gamma, \Delta) = \mu_{\alpha_0}(\Gamma)$. The space–time flow measure is defined in this way in order to make it a legitimate two-dimensional measure (i.e., so that it obeys the necessary additivity conditions) and so that Theorems 2 and 3 can be applied directly to obtain the scaling.

The generalized space–time moment of interest becomes

$$S_{n,m,\alpha_0}(h) = \sum_{\gamma|n} \sum_{\delta|m} \Pi_{\alpha_0}^h(\Gamma_{\gamma|n}, \Delta_{\delta|m}). \tag{24}$$

We now wish to use the recursive structure of the network to obtain a distributional equality. Hence, it is seen that the moment $S_{n,m,\alpha_0}(h)$ obeys

$$S_{n,m,\alpha_0}(h) \overset{d}{=} \sum_{\gamma|n} \left(\lambda_{\alpha_0}^h(\Gamma_{\gamma|n}) \prod_{i=1}^{n} W_{\gamma|i}^h\right) S_{m,\alpha_n}^{(\gamma|n)}(h),$$

where the "d" indicates equality in distribution and the $S_{m,\alpha_n}^{(\gamma|n)}$ are independent and distributed as $\sum_{\delta|m} \pi_{\alpha_n}^h(\Delta_{\delta|m})$. From this it may be shown, using the results in Theorems 2 and 3, that with probability 1

$$\lim_{n,m\to\infty} \frac{\log S_{n,m,\alpha_0}(h)}{n\chi_{\text{rain}}(h)\log b + m\chi_{\text{flow}}(h)\log c} = 1 \tag{25}$$

if $2h < h_c$ and $\chi_{\text{rain}}(2h) < 2\chi_{\text{rain}}(h)$. As above, note that the scaling behavior of $S_{n,m,\alpha_0}(h)$ does not depend on initial generator type.

Eq. (25) provides scaling of the space–time moment as *both* spatial and temporal resolutions change. We may also, however, look at scaling with respect to only temporal resolution or only spatial resolution, but, as the following discussion shows, we must be a bit careful in doing this. Consider, for example, spatial scaling. In looking at spatial scaling of flow we are typically interested in understanding how flow properties change with drainage area; i.e., drainage area becomes the scale parameter. This scaling is of much interest in regional flood studies. In the present setup, if we envision that Γ is associated with a finite region in two-dimensional space, then the area A associated with sub-region $\Gamma_{\gamma|n}$ would be proportional to $\lambda_{\alpha_0}(\Gamma_{\gamma|n})$ or to b^{-n}. Holding m fixed, it follows from (25) that $S_{n,m,\alpha_0}(h)$ scales as $A^{\theta(h)}$ with

$$\theta(h) = -\chi_{\text{rain}}(h). \tag{26}$$

Notice that in this formulation we have defined the "time" scale of the sub-region flow by subdividing the support m times over and above the n subdivisions involved in defining the size of the sub-region. The consequence is that the scale at which the sub-region flow is measured changes with sub-region size.

If it is desired on the other hand to assume that temporal measurement scale is independent of sub-region size, we must change variables from (n, m) to (n, k) where $k = m + n$; now holding k fixed to look at scaling with A yields from (25)

$$\theta(h) = -\chi_{\text{rain}}(h) + \chi_{\text{flow}}(h)/r. \tag{27}$$

Thus, the spatial scaling depends on exactly how temporal resolution is treated. More particularly, the results show that if the temporal resolution is varied proportionally with drainage area, the spatial scaling exponent would involve only the mass exponent of the rainfall (Eq. (26)), whereas if it is held constant, it would also involve the flow exponent, and hence the network.

4.3. Scaling of peak flows

Flow mass exponents may be used to look at scaling of peak flows. Consider again the moment $\sum_{\delta \mid m} \pi_{\alpha_0}^h(\Delta_{\delta \mid m})$ used to define the mass exponent in (21). It is seen that for fixed m, and hence for a fixed set of intervals $\Delta_{\delta \mid m}$, letting the moment order h grow large leads to

$$\lim_{h \to \infty} \left(\sum_{\delta \mid m} \pi_{\alpha_0}^h(\Delta_{\delta \mid m}) \right)^{1/h} = \hat{\pi}_m,$$

or, equivalently,

$$\lim_{h \to \infty} \frac{1}{h} \log \left(\sum_{\delta \mid m} \pi_{\alpha_0}^h(\Delta_{\delta \mid m}) \right) = \log(\hat{\pi}_m), \tag{28}$$

with probability 1, where $\hat{\pi}_m = \max(\pi_{\alpha_0}(\Delta_{\delta \mid m}))$; the maximum is taken over the finite set of intervals $\Delta_{\delta \mid m}$ and may occur at more than one interval, and dependence of $\hat{\pi}_m$ on initial generator is not shown. Assume that the conditions of Theorem 3(ii) hold for all positive integers h, and further that the following limit exists:

$$\lim_{h \to \infty} \frac{1}{h} \chi_{\text{flow}}(h) = \kappa < 0. \tag{29}$$

Note that this assumption implies $h_c = \infty$. It follows that with probability 1

$$\lim_{m \to \infty} \frac{\log(\hat{\pi}_m)}{m \log c} = \lim_{m \to \infty} \lim_{h \to \infty} \frac{1}{hm \log c} \log \left(\sum_{\delta \mid m} \pi_{\alpha_0}^h(\Delta_{\delta \mid m}) \right) = \lim_{h \to \infty} \frac{1}{h} \chi_{\text{flow}}(h) = \kappa. \tag{30}$$

Under these conditions, the scaling exponent for peak flows is given by the limit on the right.

Existence of the limit in (29) entails asymptotic linearity of $\chi_{\text{flow}}(h)$ as h gets large. We mention once again that for the Mandelbrot cascade, recent work [38] has established asymptotic linearity in h of the mass exponent under less stringent conditions than we assume here, so it is likely that the requirement of asymptotic linearity $\chi_{\text{flow}}(h)$ can be relaxed in looking at scaling of peak flows. This theory still needs to be worked out.

Scaling of peak flows in the space–time setting is a bit more complicated. First we note that allowing h to get large in the space–time moment (24) as was done in (28) yields the space–time peak; i.e., the space–time peak is

$$\lim_{h \to \infty} \left[\sum_{\gamma \mid n} \sum_{\delta \mid m} \Pi_{\alpha_0}^h(\Gamma_{\gamma \mid n}, \Delta_{\delta \mid m}) \right]^{1/h}. \tag{31}$$

To compute this, first a temporal peak is obtained for each sub-basin, and then the maximum of these peaks over all sub-basins is obtained. It follows from an argument like that in Eq. (30) that the scaling of the space–time peak will depend on limiting values of $(1/h)\chi_{\text{flow}}(h)$ and $(1/h)\chi_{\text{rain}}(h)$ via Eq. (25). The spatial area scaling exponent for peak flows (holding time resolution fixed) will be $\lim_{h \to \infty} \theta(h)/h$, where $\theta(h)$ is given by (26) or (27).

5. Examples: flow with beta-lognormal rainfall

5.1. Example 3. Regular networks

In this section we illustrate the implications of Theorem 3 assuming that rainfall is modeled as a beta-lognormal cascade [39]. We consider first regular networks and then average Shreve networks in the following example. Applications of this rainfall model to mesoscale data are presented in [40,41]. The distribution of the rainfall cascade generator W is given by

$$P[W = 0] = 1 - b^{-\beta} \quad \text{and} \quad P[W = W^+] = b^{-\beta},$$

where $0 \leqslant \beta < 1$ and W^+, the positive part of W, is given by

$$W^+ = b^{\beta - \sigma^2 \log b / 2 + \sigma Y},$$

taking Y to be a standard normal random variable. The rainfall mass exponent for this process is

$$\chi_{\text{rain}}(h) = (\beta - 1)(h - 1) + \frac{\sigma^2 \log b}{2}(h^2 - h)$$

and

$$h_{\text{c}} = \frac{2(1 - \beta)}{\sigma^2 \log b}.$$

Which term in (19) is the maximum depends on solutions $\tilde{h}$ of the equation $\chi_{\text{net}}(h) = r\chi_{\text{rain}}(h)$. For regular networks an explicit solution does not exist (such a solution can be found for average Shreve networks as seen in Example 4 below), so we illustrate numerical solution for a special case, the Peano network. Fig. 7 shows which term in (19) is the maximum for various values of the parameters σ^2 and β in the beta-lognormal model and for a Peano network. The values of h on the boundary between the network and rainfall regions are $\tilde{h}$. Spatial variability of rainfall increases as σ^2 increases and as β increases, with the limiting case $\sigma^2 = \beta = 0$ yielding spatially uniform rainfall. One can see in Fig. 7 the increasing tendency for flow to reflect rainfall scaling as σ^2 and β increase. The blank regions in Figs. 7(b)–(d) indicate values of h for which $h > h_{\text{c}}$. The decrease of h_{c} as σ^2 grows is seen.

An important special case of the beta-lognormal rainfall model is the so-called beta model for which $\sigma^2 = 0$; for this model, the positive part of the cascade generator W is degenerate at b^β and $\chi_{\text{rain}}(h) = (\beta - 1)(h - 1)$. It may be shown that for regular networks and beta rainfall there exists a critical value β_{c} of the parameter β, given by

$$\beta_{\text{c}} = \frac{\log \tilde{n}_{\max}}{\log b},$$

where $\tilde{n}_{\max} = \max_{0 \leqslant i \leqslant c-1} \tilde{n}_i$ is the maximum generator width function, such that (19) yields

$$\chi_{\text{flow}}(h) = \begin{cases} \chi_{\text{net}}(h) & \beta < \beta_{\text{c}}, \quad h \text{ sufficiently large.} \\ r\chi_{\text{rain}}(h) & \beta > \beta_{\text{c}}, \end{cases} \tag{32}$$
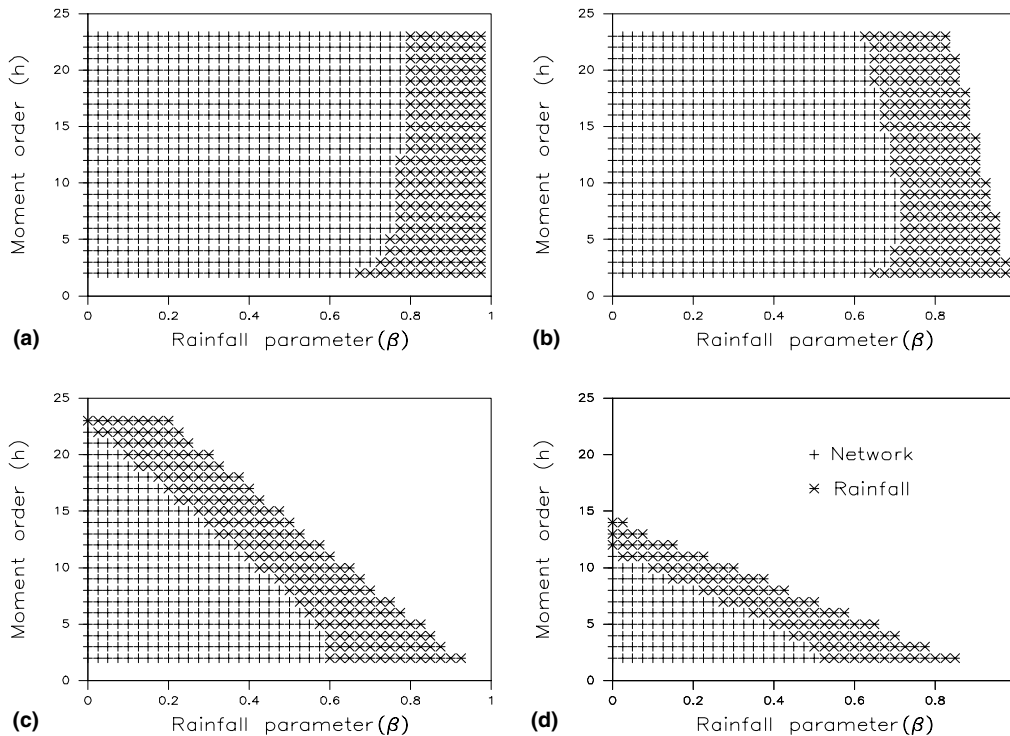

Fig. 7. Plots showing maximal term (network or rainfall) in determination of flow mass exponent for selected values of h and of beta-lognormal rainfall parameters: (a) $\sigma^2 = 0.00$, (b) $\sigma^2 = 0.01$, (c) $\sigma^2 = 0.05$, (d) $\sigma^2 = 0.10$.

β is an intermittency parameter, and (32) shows that the magnitude of this parameter determines the relative influence of rainfall and network properties on flow. When β is small, rainfall is more spatially uniform (again, the limiting case $\beta = 0$ or $W = 1$ with probability 1, yields spatially constant rainfall) and flow scaling is determined by the network. On the other hand, when rainfall is highly intermittent spatially, or when β is large, flow scaling is determined by rainfall properties. Fig. 7(a) illustrates flow scaling for beta rainfall on Peano networks. The critical value of β is $\beta_c = \log 3 / \log 4 \approx 0.79$ and the behavior in Eq. (32) is clearly seen.

A simulation experiment was carried out to illustrate these results for the beta rainfall model and a regular recursive replacement network with branching number $b = 3$, $c = 2$, and generator width function $\tilde{n}_1 = 1$, $\tilde{n}_2 = 2$. Five hundred realizations of a random rainfall field were generated using each of the three rainfall parameter values ($\beta = 0.20$, 0.40, and 0.90), and flows at the outlet of the network computed in each case. The multiplicative rainfall cascade was generated down to 11 levels, so the instantaneous unit hydrograph (the measure π) is approximated by π_m with $m = 11$. The critical rainfall parameter value for this network is $\beta_c = \log 2 / \log 3 \approx 0.63$. Fig. 8 shows cumulative flow for a single rainfall realization for each value of β. The uniform rainfall curve is the cumulative width function (measure ρ) or flow with rainfall parameter $\beta = 0$. The shape of the flow measure for $\beta = 0.90$ indicates that rainfall intermittency is high in this case, and rainfall is non-zero over only a small portion of the basin.

Fig. 9 shows plots of $\chi_{net}(h)$, $r\chi_{rain}(h)$, and the average value (for the 500 realizations) of $\tau_{flow}(h)$ estimated by Eq. (22), again computed using rainfall generated down to 11 levels. Also shown are lower and upper 95% confidence limits indicating uncertainty in these average values. The lower and upper limits nearly coincide for $\beta = 0.20$, but uncertainty becomes greater as β increases, showing that increased rainfall intermittency tends to make estimation of the mass exponent more problematic. The plots show agreement with the behavior predicted in Theorem 3. That is, the average $\tau_{flow}(h)$ is close to $\chi_{net}(h)$ for $\beta = 0.20$ and 0.40, which are less than the critical value β_c, and on the other hand $\tau_{flow}(h)$ is near $r\chi_{rain}(h)$ for $\beta = 0.90$, which is greater than β_c. It is interesting, however, that $\chi_{net}(h)$ does lie just outside the flow mass exponent confidence limits for $\beta = 0.40$, revealing a small bias that is being caused by generating rainfall and the network only down to 11 levels. This bias would be diminished with simulations down to finer scales, although it appears that the number of levels needed to make the bias negligible increases as β gets nearer β_c.

We next provide a comparison of our results with those of Gupta et al. [20], where results were presented for area scaling of peak flows resulting from beta rainfall on a Peano basin. Thus, in their study, attention is focused on $\theta(h)$ for large h. Before comparing results, however, we wish to briefly discuss some minor differences in approach. First, as in our development of space–time flow scaling above, they looked at flows from sub-regions. One difference, however, is that in Eq. (23) we define the space–time flow for *all* sub-regions $\Gamma_{\gamma|n}$ in the basin Γ, whereas they consider only flows from sub-regions that are complete drainage basins, i.e., those that receive no upstream flow from other sub-regions. Thus, to make our approach identical to theirs, the sum over all spatial sub-regions in Eq. (24) would need to be replaced by a sum over only sub-regions that are complete drainage basins. It can be shown that the development would carry through in essentially the same manner if this change were made, with no change in the scaling exponent (27). A second difference is that rather than looking at space–time peaks as in Eq. (31), they compute peaks at spatial points and then looked at scaling of the spatial average of these peaks to the h power. That is, in terms of the notation in this paper, they looked at essentially
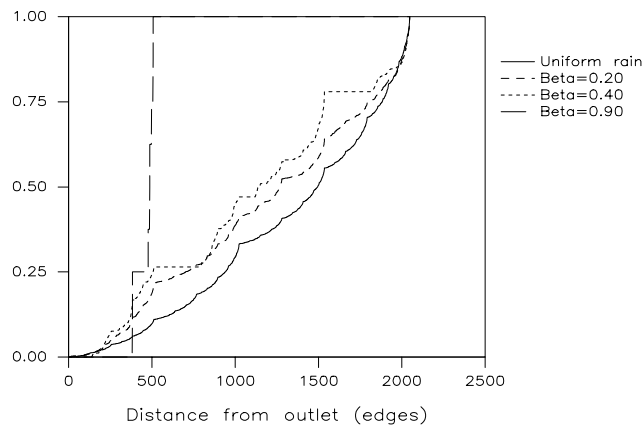

Fig. 8. Plot showing cumulative flow from a recursive replacement network with simulated β-model rainfall for several values of the parameter β.
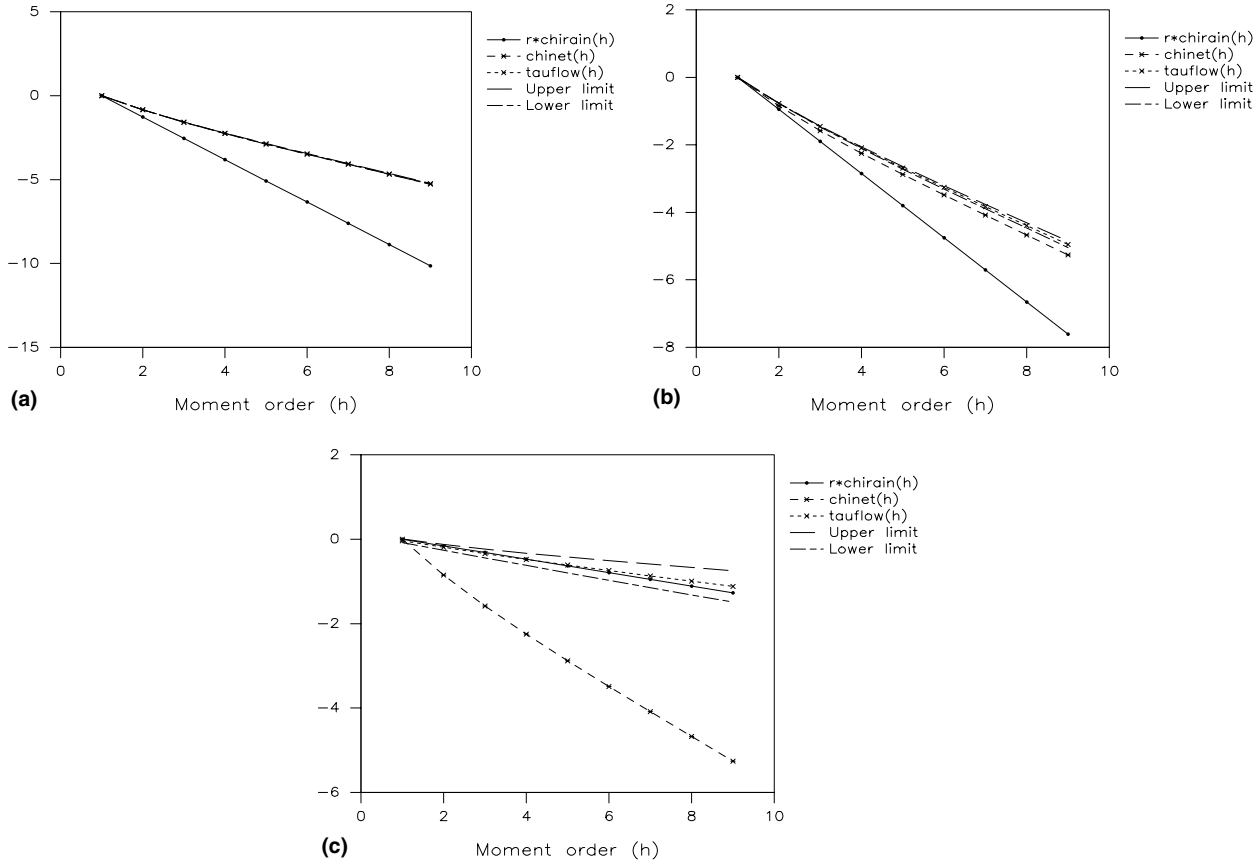
Fig. 9. Plots showing $\chi_{net}(h)$, $r\chi_{rain}(h)$, an estimate of $\tau_{flow}(h)$ obtained by taking an average value for 500 realizations of β-rainfall ((a) $\beta = 0.20$, (b) $\beta = 0.40$, and (c) $\beta = 0.90$) generated down to 11 levels, and 95% confidence limits for this estimate.

$$\sum_{\gamma\,|\,n} \left\{ \lim_{h'\to\infty} \left[\sum_{\delta\,|\,m} \Pi_{\alpha_0}^{h'}(\Gamma_{\gamma\,|\,n}, \Delta_{\delta\,|\,m}) \right]^{1/h'} \right\}^h. \tag{33}$$

However, observe that taking this expression to the $1/h$ power and letting h get large yield the same limit as (31). Thus the large h behavior of (33) will also provide the scaling exponent of the space–time maximum.

Our result for the area scaling exponent of the space–time peak for beta rainfall on regular channel networks is

$$\lim_{h\to\infty} \frac{\theta(h)}{h} = 1 - \beta$$

if (26) is used for $\theta(h)$, and

$$\lim_{h\to\infty} \frac{\theta(h)}{h} = \begin{cases} \frac{\log \tilde{n}_{max}}{\log b} - \beta, & \beta < \beta_c, \\ 1, & \beta > \beta_c \end{cases} \tag{34}$$

if (27) is used. The expression of Gupta et al. [20] for the scaling exponent for (33) is $h(\log 3/\log 4 - \beta) + \beta$. The limit of $1/h$ times this expression as h gets large is $\log 3/\log 4 - \beta$, which is the space–time scaling exponent. In their study, temporal measurement scale was taken to be independent of sub-region size, and $\beta \leqslant 0.5$, so (34) with $\beta < \beta_c$ is the relation of interest. Agreement of the two results is seen by noting $\tilde{n}_{max} = 3$, $b = 4$ for the Peano basin.

5.2. Example 4. Average Shreve channel networks

We now consider beta-lognormal rainfall on an average Shreve network. For the average Shreve network $\chi_{net}(h) = 1 - h$, from Example 2. The solution to $\chi_{net}(h) = r\chi_{rain}(h)$ is

$$\tilde{h} = \tilde{h}(\beta, \sigma^2) = \frac{1 - 2\beta}{\sigma^2 \log 4};$$

note that $\tilde{h} < h_c$ if $\sigma^2 > 0$. Thus,

$$\chi_{\text{flow}}(h) = \begin{cases} \chi_{\text{net}}(h), & \tilde{h} \geqslant 1, \ h < \tilde{h}, \\ r\chi_{\text{rain}}(h), & \tilde{h} \geqslant 1, \ h \geqslant \tilde{h} \text{ or } \tilde{h} < 1. \end{cases}$$

When $\sigma^2 = 0$ (beta rainfall model), $\tilde{h} = \pm\infty$, with sign determined by the value of the rainfall parameter β. There is again (as in Example 3) a critical value ($=1/2$) of β such that

$$\chi_{\text{flow}}(h) = \begin{cases} \chi_{\text{net}}(h), & \beta < 1/2, \\ r\chi_{\text{rain}}(h), & \beta > 1/2. \end{cases}$$

An important conclusion of this example is that even for networks for which the width function does not exhibit multifractality the flow may reflect either the rainfall or the network properties, depending on the degree of spatial variability in the rainfall.

6. Discussion, conclusions, and prospects

We have computed the scaling exponents of the moments of the flow response at the outlet to instantaneous multifractal rainfall on a wide class of recursively generated self-similar trees and applied these results to compute the space–time flows throughout the network and their peaks, generalizing the results of Gupta et al. [20]. The applicability of these results to actual flows in river basins is not direct, but given observations of approximate scale invariance in rainfall and river networks, they can be viewed as a building block in developing a physical–statistical space–time theory of streamflow. As discussed by Gupta et al. [20], this theory has relevance to the problem of estimation of flood frequencies at ungauged locations by regionalization, but also, perhaps more importantly, provides predictions regarding the space–time structure of streamflow, a hitherto mostly unexamined topic that nevertheless should lie at the heart of river basin hydrology, and which would allow predictions of other important relevant quantities such as the spatial extent of floods of various frequencies.

To further develop such a theory, and one that is realistic enough to make predictions that can be tested with data, additional developments are clearly needed. In the present framework, extension to properties of flows from space–time rainfall (e.g., [30,41]) is the obvious next step. The effects of spatially variable runoff generation and routing of flows through the network are the most important physical processes not considered. One may also consider in further detail the accuracy of the scale invariant models of river networks and rainfall used here. Recent research has shown that observed network width functions are generally not multifractal [46,63]. However this does not preclude the self-similarity of the trees themselves, as for example in the case of the average Shreve tree discussed here. Development of random versions of self-similar tree models [4,9,62] should prove to be much more realistic, and it should not present great difficulty to extend the present results to them.

Regarding rainfall, further testing and development of multifractal models is clearly needed. For one thing, it is somewhat controversial whether (or at what length scales) spatial rain itself can be regarded as a multifractal. We assumed this here, as was argued by Over and Gupta [40,41] using tropical oceanic data at a 4 km minimum spatial scale. The alternative is whether it should be considered in some sense a smoothed multifractal field (e.g., [32,52]). Interestingly, temporal rain at relatively short, but not very short, time scales (from a few hours to a few days) appears to generally satisfy multifractal criteria (e.g., [12,16,53]). Furthermore, rainfall scaling properties seem to depend on large-scale average rainrate [40], atmospheric conditions [44], and location and time of year [37]. Combining these observations into a realistic space–time model is still to be accomplished.

Despite these challenges, the present results give an indication of the form a space–time theory of streamflow might take and of the feasibility of such a project. Current concerns such as those regarding the possible effect of climate change on hydrologic extremes (e.g., [56]) make such research all the more important.

Appendix A

Proof of Theorem 1. It is desired to look at behavior of moments defined by

$$\sum_{\delta \mid m} \rho_{\alpha_0}^h (\Delta_{\delta \mid m}) = \sum_{\delta_0, \ldots, \delta_m} \rho_{\alpha_0}^h (\Delta_{\delta_0, \ldots, \delta_m}).$$

Toward this end, define the quantity

$$U_m(\eta_0(h)) = \sum_{\delta_1,\ldots,\delta_m} \sum_{i=1}^{h} \rho_{\alpha_0(i)}(\Delta_{\delta_0(i),\delta_1,\ldots,\delta_m}),$$

where $\eta_0(h)$ stands for the $2h \times 1$ vector $\delta_0(1), \alpha_0(1); \delta_0(2), \alpha_0(2); \ldots; \delta_0(h), \alpha_0(h)$. From Eq. (12) it may be shown that

$$U_m(\eta_0(h)) = \sum_{\eta_0'(h)} \sum_{\delta_1} \prod_{i=1}^{h} \phi(\alpha_0(i), \alpha_0'(i)) n_{\delta_0(i)c+\delta_1-\delta_0'(i)}(\alpha_0(i), \alpha_0'(i)) U_{m-1}(\eta_0'(h)).$$

Each δ_0 may take on c^* values and each α_0 may take on two values (I or E), so the $U_m(\eta_0(h))$ may be arranged to form a $(2c^*)^h \times 1$ vector, U_m, which obeys

$$U_m = \frac{1}{b^h} CA(h)C^{-1}U_{m-1}, \tag{A.1}$$

with matrix C a diagonal matrix with diagonal elements $\prod_{i=1}^{h} C(\alpha_0(i))$ and $A(h)$ is as defined in Theorem 1. From (A.1) the vector U_m will scale asymptotically (for large m) as the maximum eigenvalue $\omega(h)$ of $A(h)$, from which

$$\sum_{\delta\,|\,m} \rho_{\alpha_0}^{h}(\Delta_{\delta\,|\,m}) \sim k\left(\frac{\omega(h)}{b^h}\right)^m, \quad m \to \infty,$$

where k is a constant independent of m. The result in Theorem 1 then follows. $\square$

Proof of Theorem 2. This theorem may be proven in much the same way as the corresponding result for Mandelbrot cascades is proven by Holley and Waymire [21, Theorem 2.7]. The key step is to determine convergence of the sum in (17) with μ_{n,α_0}, replacing μ_{α_0}, so we shall demonstrate this step in some detail. This sum may be partitioned as

$$\sum_{\gamma\,|\,n} \mu_{n,\alpha_0}^{h}(\Gamma_{\gamma\,|\,n}) = R_{n,h,\alpha_0}(I) + R_{n,h,\alpha_0}(E), \tag{A.2}$$

where

$$R_{n,h,\alpha_0}(\zeta) = \sum_{\substack{\gamma\,|\,n \\ \alpha_n=\zeta}} \mu_{n,\alpha_0}^{h}(\Gamma_{\gamma\,|\,n})$$

and where ζ takes on the two values I (interior) and E (exterior). Thus, we are conditioning on the edge type at level n. If the two components on the right-hand side of Eq. (A.2) are written as a 2-vector R_{n,h,α_0}, it is straightforward to show that

$$E(R_{n,h,\alpha_0}\,|\,\mathscr{F}_{n-1}) = \frac{EW^h}{b^h} C_h^{-1} N C_h R_{n-1,h,\alpha_0},$$

where $\{\mathscr{F}_n\}$ is the sequence of σ-subfields of $\mathscr{F}$ defined by

$$\mathscr{F}_n = \sigma\{W(\gamma\,|\,j) : (\gamma\,|\,j) \in \Gamma(j),\ 1 \leqslant j \leqslant n\},$$

C_h is a 2×2 diagonal matrix with diagonal elements $C^{-h}(I)$ and $C^{-h}(E)$, and N is the 2×2 matrix $\{n(\alpha', \alpha)\}$. We invoke the diagonability theorem [48, p. 284] to show that there exists a non-singular matrix A such that $N = A^{-1}\Lambda A$, where Λ is diagonal with elements b' and b, the eigenvalues of N. The sub-martingale convergence theorem may then be used to establish that there exist random variables Y_1 and Y_2 such that, almost surely,

$$\frac{a_1^{\mathrm{T}} R_{n,h,\alpha_0}}{\left(\frac{EW^h}{b^h}\right)^n b'^n} \to Y_1, \quad \frac{a_2^{\mathrm{T}} R_{n,h,\alpha_0}}{\left(\frac{EW^h}{b^h}\right)^n b^n} \to Y_2,$$

where a_i^{T} is the ith row of AC_h. Because $b \geqslant b'$, it follows from (A.2) that there is a random variable Y such that almost surely

$$\frac{\sum_{\gamma\,|\,n} \mu_{n,\alpha_0}^{h}(\Gamma_{\gamma\,|\,n})}{\left(\frac{EW^h}{b^{h-1}}\right)^n} \to Y. \quad \square$$

Proof of Theorem 3.

(A) Proof of (ii) for the regular case

Because the proof for the regular case and the general case are very similar, we simplify the presentation by first giving the detailed proof for the regular case and then outline how the extension to the general case proceeds. We

consider initially part (ii) of Theorem 3, and we first look at convergence of measures $\pi_n = \mu_n d^{-1}$. (We drop the subscript indicating initial generator α_0, as this is fixed at E.) Define the set Q of $h \times h$ matrices for which $M = (m_{ij}) \in Q$ obeys (1) $m_{ii} = 1$; (2) $m_{ij} = 0$ or 1 for $i \neq j$; (3) $m_{ij} = m_{ji}$ (symmetry); and (4) $m_{ij} = 1$ and $m_{ik} = 1$ implies $m_{jk} = 1$. Next for $\Gamma(n) =$ the set of curtailed sequences $(\gamma|n)$, define the mapping $z_n : \Gamma(n)^h \to Q$ by

$$(z_n(\gamma^{(1)}|n, \gamma^{(2)}|n, \ldots, \gamma^{(h)}|n))_{ij} = \begin{cases} 0, & \gamma^{(i)}|n \neq \gamma^{(j)}|n, \\ 1, & \gamma^{(i)}|n = \gamma^{(j)}|n. \end{cases}$$

We see that we may write

$$\sum_{\delta|n} \pi_n^h(\Delta_{\delta|n}) = \sum_{M \in Q} S_n(M),$$

where

$$S_n(M) = \sum_{\delta|n} {\sum}^* \mu_n(\Gamma_{\gamma^{(1)}|n}) \mu_n(\Gamma_{\gamma^{(2)}|n}) \cdots \mu_n(\Gamma_{\gamma^{(h)}|n}), \tag{A.3}$$

and where $\sum^*$ denotes a sum over $\gamma^{(1)}|n, \gamma^{(2)}|n, \ldots, \gamma^{(h)}|n$ obeying $f(\gamma_j^{(i)}) = \delta_j$, $1 \leqslant i \leqslant h$, $1 \leqslant j \leqslant n$ and $z_n(\gamma^{(1)}|n, \gamma^{(2)}|n, \ldots, \gamma^{(h)}|n) = M$. The index set for the summation $\sum^*$ may be empty, in which case $S_n(M)$ is defined to be zero. (It may be shown that a sufficient condition for the index set to be non-empty for any M is $n \geqslant \log h / \log \tilde{n}_{\max}$.)

With each matrix M associate an $h \times 1$ vector $k = k(M) = (k_j(M))$ where $k_j(M)$ is j^{-1} times the number of rows in M summing to j. The vectors k assume values in the set $J(h)$ defined by

$$J(h) = \left\{ k = (k_1, k_2, \ldots, k_h) : k_j \in \{0, \ldots, h\}, \sum jk_j = h \right\},$$

and they play the role of defining the number of sets of matching indices in a multiple summation. It is now readily shown from the definition of $S_n(M)$ that

$$E[S_n(M) \,|\, \mathscr{F}_{n-1}] = \left(\frac{1}{b^h} \prod_{j=1}^{h} E^{k_j(M)} W^j \right) \sum_{M' \in Q} c(M, M') S_{n-1}(M'),$$

where $c(M, M') = \sum_{\delta_n} \sum^{**} 1$ with $\sum^{**}$ denoting a sum over $\gamma_n^{(1)}, \gamma_n^{(2)}, \ldots, \gamma_n^{(h)}$ obeying $f(\gamma_n^{(i)}) = \delta_n$, $1 \leqslant i \leqslant h$, $z_n(\gamma^{(1)}|n, \gamma^{(2)}|n, \ldots, \gamma^{(h)}|n) = M$ and $z_{n-1}(\gamma^{(1)}|n-1, \gamma^{(2)}|n-1, \ldots, \gamma^{(h)}|n-1) = M'$. The constants $c(M, M')$ do not depend on n.

We order the elements $k \in J(h)$ as follows: Let $k, k' \in J(h)$, and define $l = min\{j : k_m = k'_m, \ j < m \leqslant h\}$; let $l = h$ if this set is empty. Then we say that $k' < k$ if $k'_l < k_l$. This ordering in turn induces an ordering on matrices $M \in Q$; for two matrices M and M' for which $k(M) = k(M')$, we may use any arbitrary rule for ordering M and M'. We then arrange the $S_n(M)$ to form a vector, say S_n, based on this ordering. Observe that $c(M, M') = 0$ if $M' < M$ and

$$c(M, M) = \sum_{i=0}^{c-1} \tilde{n}_i^{\sum k_j(M)} = \omega\left(\sum k_j(M) \right).$$

Thus, we have

$$E[S_n \,|\, \mathscr{F}_{n-1}] = TS_{n-1}, \tag{A.4}$$

where T is an upper triangular matrix with diagonal elements given by

$$\lambda_{k(M)} = \frac{1}{b^h} \prod_{j=1}^{h} E^{k_j(M)} W^j \omega\left(\sum k_j(M) \right). \tag{A.5}$$

We may again invoke the diagonability theorem to show that there exists a non-singular matrix B such that

$$T = B^{-1} \Lambda B,$$

where Λ is the diagonal matrix with elements $\lambda_{k(M)}$, the eigenvalues of T. From this it follows that

$$E[BS_n \,|\, \mathscr{F}_{n-1}] = \Lambda BS_{n-1}.$$

The sub-martingale convergence theorem may then be used to establish that there exist random variables Y_M such that, almost surely,

$$\frac{b_M^T S_n}{\lambda_{k(M)}^n} \to Y_M,$$

letting b_M^T be the Mth row of B. From this it follows that there is a random variable Y such that, almost surely,

$$\frac{\sum_{\delta|n} \pi_n^h(\Delta_{\delta|n})}{\tilde{\lambda}(h)^n} \to Y, \tag{A.6}$$

where $\tilde{\lambda}(h)$ is defined by

$$\tilde{\lambda}(h) = \max_{k \in J(h)} (\lambda_k). \tag{A.7}$$

We next prove that

$$\tilde{\lambda}(h) = \max(\lambda_{\underline{k}}, \lambda_{\overline{k}}),$$

where $\overline{k} = (h, 0, \ldots, 0)$ and $\underline{k} = (0, \ldots, 0, 1)$, from which it follows that

$$\tilde{\lambda}(h) = c^{\max[\chi_{net}(h), r\chi_{rain}(h)]}.$$

We wish to show that the maximum in (A.7) occurs at one of the two elements $\underline{k}$ or $\overline{k}$ in $J(h)$. Consider

$$s(k) = \chi_{net}\left(\sum k_j\right) + r\sum k_j \chi_{rain}(j), \quad k \in J(h),$$

and let $w_j = jk_j/h$, giving $\sum w_j = 1$. Then

$$s(k) = \chi_{net}\left(\sum w_j \frac{h}{j}\right) + r\sum w_j \frac{h}{j} \chi_{rain}(j) \leqslant \sum w_j \chi_{net}\left(\frac{h}{j}\right) + r\sum w_j \frac{h}{j} \chi_{rain}(j) = \sum w_j g(j) \tag{A.8}$$

using the convexity of χ_{net} and defining

$$g(x) = \chi_{net}\left(\frac{h}{x}\right) + \frac{rh}{x}\chi_{rain}(x).$$

It is readily shown using convexity of χ_{net} and χ_{rain} that

$$\sup_{1 \leqslant x \leqslant h} g(x) = \max[g(1), g(h)],$$

and therefore using the constraints $0 \leqslant w_j \leqslant 1$ and $\sum w_j = 1$ we have

$$\sum w_j g(j) \leqslant \max[g(1), g(h)] = \max[\chi_{net}(h), r\chi_{rain}(h)].$$

The fact that $s(k)$ in (A.8) coincides with these two extreme points of $\sum w_j g(j)$ for $k = \underline{k}$ and $k = \overline{k}$ proves the desired result.

Finally, we return to looking at π rather than π_n. The result in the theorem follows from demonstrating existence of a random variable $\tilde{Y}$ such that

$$\frac{\sum_{\delta|n} \pi^h(\Delta_{\delta|n})}{\tilde{\lambda}(h)^n} \to \tilde{Y}, \quad \text{almost surely.}$$

Existence of such a variable follows from (A.6) together with assumptions that $2h < h_c$ and

$$\frac{\tilde{\lambda}(2h)}{\tilde{\lambda}(h)^2} < 1, \tag{A.9}$$

using a line of reasoning very similar to that used by Holley and Waymire [21] in the proof of their Theorem 2.7; details will be omitted here. Condition in (A.9) is seen to be identical to the condition $\chi_{flow}(2h) < 2\chi_{flow}(h)$, which reduces to the condition $r\chi_{rain}(2h) < 2\chi_{flow}(h)$ in the hypothesis of the theorem if it is noted that $\chi_{net}(2h) < 2\chi_{net}(h)$ always holds for the deterministic recursive replacement tree. This concludes the proof of part (ii) of Theorem 3 for regular networks.

(B) *Proof of* (i) *for the regular case*

The result in part (i) of the theorem involving convergence of the expectation follows directly from what has been done. Convergence of $ES_n/\tilde{\lambda}(h)^n$ to a finite limit may be shown by taking expectations in (A.4), and the result in the theorem follows readily by writing

$$E \sum_{\delta \mid n} \pi^h(\Delta_{\delta \mid n}) = \mu_Z^{\mathrm{T}} E S_n,$$

where μ_Z is the vector with Mth element $E \prod_{i=1}^{h} z_{\gamma^{(i)} \mid n}$ subject to $Z_n(\gamma^{(1)} \mid n, \gamma^{(2)} \mid n, \ldots, \gamma^{(h)} \mid n) = M$.

(*C*) *Proof for the general case*

For the general case, rather than $S_n(M)$ in (A.3), we must consider, for $\theta_i \in \{0, 1, \ldots, c^* - 1\}$ and $\zeta \in \{I, E\}$,

$$S_{n, \alpha_0}(M; \theta_1, \ldots, \theta_h; \zeta_1, \ldots, \zeta_h) = \sum_{\delta \mid n} \sum{}^* \mu_{n, \alpha_0}(\Gamma_{\gamma^{(1)} \mid n}) \mu_{n, \alpha_0}(\Gamma_{\gamma^{(2)} \mid n}) \cdots \mu_{n, \alpha_0}(\Gamma_{\gamma^{(h)} \mid n}) \tag{A.10}$$

where now $\sum^*$ denotes a sum over $\gamma^{(1)} \mid n, \gamma^{(2)} \mid n, \ldots, \gamma^{(h)} \mid n$, with $\gamma_j^{(i)} = (\alpha_j^{(i)}, \upsilon_j^{(i)})$, subject to

$$\alpha_n^{(i)} = \zeta_i, \quad 1 \leqslant i \leqslant h,$$

$$g_n(f(\upsilon_1^{(i)}; \alpha_0, \alpha_1^{(i)}), \ldots, f(\upsilon_{n-1}^{(i)}; \alpha_{n-2}^{(i)}, \alpha_{n-1}^{(i)}), f(\upsilon_n^{(i)}; \alpha_{n-1}^{(i)}, \zeta_i) + \theta_i) = (\delta_0, \ldots, \delta_n), \quad 1 \leqslant i \leqslant h,$$

and

$$z_n(\gamma^{(1)} \mid n, \gamma^{(2)} \mid n, \ldots, \gamma^{(h)} \mid n) = M;$$

the function z_n was defined above and the function g_n is defined as follows. For any n non-negative integers $i_1, i_2, \ldots, i_n$, $(j_0, j_1, \ldots, j_n) = g_n(i_1, i_2, \ldots, i_n)$ are the $n + 1$ unique non-negative integers obeying the constraint $j_k \in \{0, 1, \ldots, c - 1\}$, $1 \leqslant k \leqslant n$, (note that j_0 is not so constrained) such that

$$\sum_{k=1}^{n} i_k c^{-k} = \sum_{k=0}^{n} j_k c^{-k}.$$

In other words, the fractional part of the number on the left is represented in base c form on the right. Given M, we define this quantity only for certain values of ζ_i and θ_i; the constraint is imposed that $m_{ij} = 1$ implies $\zeta_i = \zeta_j$ and $\theta_i = \theta_j$. Thus, given M there are $(2c^*)^{\sum k_j(M)}$ random variables. If we again arrange (ordering based on M as above) all these variables to form a vector which we shall denote by S_{n, α_0}, it may be shown that

$$E[S_{n, \alpha_0} \mid \mathscr{F}_{n-1}] = T S_{n-1, \alpha_0},$$

where now the matrix T is upper block triangular with Mth diagonal matrix (size $(2c^*)^{\sum k_j(M)}$ by $(2c^*)^{\sum k_j(M)}$) given by

$$\left(\prod_{i=1}^{h} E^{k_i(M)} W^i \prod_{i=1}^{\sum k_j(M)} \phi^{ik_i(M)}(\zeta_i, \zeta_i') \sum_{\delta_1} \prod_{i=1}^{\sum k_j(M)} n_{\theta_i c + \delta_1 - \theta_1'}(\zeta_i, \zeta_i') \right).$$

It is recognized from the definition of $A(h)$ in Theorem 1 that the maximum eigenvalue of this matrix is again given by expression (A.5), where now $\omega(\sum k_j(M))$ is the maximum eigenvalue of $A(\sum k_j(M))$. The remainder of the argument is similar to that for regular networks. $\square$

References

[1] Barndorff-Nielsen OE, Gupta VK, Perez-Abreu V, Waymire E, editors. Stochastic methods in hydrology: rain, landforms, and floods. Advanced series on statistical science and probability, vol. 7. Singapore: World Scientific; 1998.

[2] Barnsley M. Fractals everywhere. New York: Academic Press; 1988.

[3] Burd GA, Waymire EC. Independent random cascades on the Galton–Watson trees. Proc Ann Math Soc 2000;128:2753–61.

[4] Burd GA, Waymire EC, Winn RD. A self-similar invariance of critical binary Galton–Watson trees. Bernoulli 2000;6(1):1–21.

[5] Carsteanu A, Venugopal V, Foufoula-Georgiou E. Event-specific multiplicative cascade models and an application to rainfall. J Geophys Res 1999;104(D24):31611–22.

[6] Chow VT, Maidment DR, Mays LW. Applied hydrology. New York: McGraw-Hill; 1988.

[7] Cieplak M, Giacometti A, Maritan A, Rinaldo A, Rodriguez-Iturbe I, Banavar JR. Models of fractal river basins. J Statist Phys 1998;91:1–15.

[8] Claps P, Fiorentino M, Oliveto G. Informational entropy of fractal river networks. J Hydrol 1996;187:145–56.

[9] Cui G, Williams B, Kuczera G. A stochastic Tokunaga model for stream networks. Water Resour Res 1999;35:3139–47.

[10] Deidda R. Multifractal analysis and simulation of rainfall fields in space. Phys Chem Earth (B) 1999;24:73–8.

[11] Dodds PS, Rothman DH. Unified view of scaling laws for river networks. Phys Rev E 1999;59(5A):4865–77.

[12] Fabry F. On the determination of scale ranges for precipitation fields. J Geophys Res 1996;101(D8):12819–26.

[13] Feder J. Fractals. New York: Plenum Press; 1988.

[14] Flajolet P, Prodinger H. Level number sequences for trees. Disc Math 1987;65:149–56.

[15] Flammini A, Colaiori F. Exact analysis of the Peano basin. J Phys A 1996;29:6701–8.

[16] Fraedrich K, Larnder C. Scaling regimes of composite rainfall time series. Tellus 1993;45A:289–98.

[17] Gupta VK, Waymire E. On the formulation of an analytical approach to hydrologic response and similarity at the basin scale. J Hydrol 1983;65:95–124.

[18] Gupta VK, Waymire EC. Multiscaling properties of spatial rainfall and river flow distributions. J Geophys Res 1990;95:1999–2009.
[19] Gupta VK, Waymire EC. A statistical analysis of mesoscale rainfall as a random cascade. J Appl Meteor 1993;32:251–67.
[20] Gupta VK, Castro SL, Over TM. Scaling exponents of spatial peak flows from rainfall and river network geometry. J Hydrol 1996;187:81–104.
[21] Holley R, Waymire E. Multifractal dimensions and scaling exponents for strongly bounded random cascades. Ann Appl Probab 1992;2:819–45.
[22] Kahane JP, Peyrière J. Sur certaines martingales de Benoit Mandelbrot. Adv Math 1976;22:131–45.
[23] Kirkby MJ. Tests of the random model and its application to basin hydrology. Earth Surf Proc Landforms 1976;1:197–212.
[24] Kumar P, Foufoula-Georgiou E. A multicomponent decomposition of spatial rainfall fields, 2. Self-similarity in fluctuations. Water Resour Res 1993;29(8):2533–44.
[25] Lovejoy S, Schertzer D. Multifractals, universality classes, and satellite and radar measurements of cloud and rain fields. J Geophys Res 1990;95:2021–34.
[26] Mandelbrot BB. The fractal geometry of nature. New York: Freeman; 1983.
[27] Marani A, Rigon R, Rinaldo A. A note on fractal channel networks. Water Resour Res 1991;27:3041–50.
[28] Marani M, Rinaldo A, Rigon R, Rodriguez-Iturbe I. Geomorphological width functions and the random cascade. Geophys Res Lett 1994;21:2123–6.
[29] Maritan A, Rinaldo A, Rigon R, Giacometti A, Rodriguez-Iturbe I. Scaling laws for river networks. Phys Rev E 1996;53(2):1510–5.
[30] Marsan D, Schertzer D, Lovejoy S. Causal space–time multifractal processes: predictability and forecasting of rain fields. J Geophys Res 1996;101(D21):26333–46.
[31] Meakin P, Feder J, Jossang T. Simple statistical models for river networks. Physica A 1991;176:409–29.
[32] Menabde M, Seed A, Harris D, Austin G. Self-similar random fields and rainfall simulation. J Geophys Res 1997;102(D12):13509–15.
[33] Molchan GM. Scaling exponents and multifractal dimensions for independent random cascades. Commun Math Phys 1996;179:681–702.
[34] Molchan GM. Turbulent cascades: limitations and a statistical test of the lognormal hypothesis. Phys Fluids 1997;9(8):2387–96.
[35] Newman WI, Turcotte DL, Gabrielov AM. Fractal trees with side branching. Fractals 1997;5:603–14.
[36] Olsson J. Limits and characteristics of the multifractal behavior of high-resolution rainfall time series. Nonlinear Processes Geophys 1995;2:23–9.
[37] Onof D, Mackay NG, Oh L, Wheater HS. An improved rainfall disaggregation technique for GCMs. J Geophy Res 1998;103(D16):19577–86.
[38] Ossiander M, Waymire E. Statistical estimation for multiplicative cascades. Ann Statist 2000;28(6):1533–60.
[39] Over TM. Modeling space–time rainfall at the mesoscale using random cascades. PhD Dissertation, Program in Geophysics, University of Colorado, 1995.
[40] Over TM, Gupta VK. Statistical analysis of mesoscale rainfall: dependence of random cascade generator of the large-scale forcing. J Appl Meteor 1994;33:1526–42.
[41] Over TM, Gupta VK. A space–time theory of mesoscale rainfall using random cascades. J Geophys Res 1996;101:26319–31.
[42] Pandey G, Lovejoy S, Schertzer D. Multifractal analysis of daily river flows including extremes for basins of five to two million square kilometres, one day to 75 years. J Hydrol 1998;208:62–81.
[43] Peckham SD. New results for self-similar trees with applications to river networks. Water Resour Res 1995;31:1023–30.
[44] Perica S, Foufoula-Georgiou E. Linkage of scaling and thermodynamic parameters of rainfall: results from midlatitude mesoscale convective systems. J Geophys Res 1996;101(D3):7431–48.
[45] Rodriguez-Iturbe I, Rinaldo A, Rigon R, Bras RL, Marani A, Ijjasz-Vasquez E. Energy dissipation, runoff production, and the three-dimensional structure of river basins. Water Resour Res 1992;28:1095–103.
[46] Rodriguez-Iturbe I, Rinaldo A. Fractal river basins, chance and self-organization. Cambridge: Cambridge University Press; 1997.
[47] Schertzer D, Lovejoy S, Lavallee D. Generic multifractal phase transitions and self-organized criticality. In: Perdang JM, Lejeume A, editors. Cellular automata: prospects in astrophysical applications. Singapore: World Scientific; 1993.
[48] Searle SR. Matrix algebra useful for statistics. New York: Wiley; 1982.
[49] Shreve RL. Infinite topologically random channel networks. J Geol 1967;75:178–86.
[50] Shreve RL. Stream lengths and basin areas in topologically random channel networks. J Geol 1969;77:397–414.
[51] Sun T, Meakin P, Jossang T. Minimum energy model for river basin geometry. Phys Rev E 1994;49:4865–72.
[52] Tessier Y, Lovejoy S, Schertzer D. Universal multifractals: theory and observations for rain and clouds. J Appl Meteor 1993;32:223–50.
[53] Tessier Y, Lovejoy S, Hubert P, Schertzer D, Pecknold S. Multifractal analysis and modeling of rainfall and river flows and scaling, causal transfer functions. J Geophys Res 1996;101(D21):26427–40.
[54] Tokunaga E. The composition of drainage networks in Toyohira river basin and valuation of Horton's first law. Geophys Bull Hakkaido Univ 1966;15:1–19.
[55] Tokunaga E. Consideration on the composition of drainage networks and their evolution. Geographical Report of Tokyo Metropolitan University, no. 13 1978.
[56] Trenberth KE. Conceptual framework for changes of extremes of the hydrological cycle with climate change. Climatic Change 1999;42:327–39.
[57] Troutman BM, Karlinger MR. Unit hydrograph approximations assuming linear flow through topologically random channel networks. Water Resour Res 1985;21:743–54.
[58] Troutman BM, Karlinger MR. Inference for a generalized Gibbsian distribution on channel networks. Water Resour Res 1994;30:2325–38.
[59] Troutman BM, Karlinger MR. Spatial channel network models in hydrology. In: Barndorff-Nielsen OE, Gupta VK, Perez-Abreu V, Waymire E, editors. Stochastic methods in hydrology: rainfall, landforms, and floods. Advanced series on statistical sciences and applied probability, vol. 7. Singapore: World Scientific; 1998.
[60] Troutman BM, Vecchia AV. Estimation of Rényi exponents in random cascades. Bernoulli 1999;5(2):191–207.
[61] Veitzer S. A theoretical framework for understanding river networks: connecting topology, process, and geometry across many scales. PhD Dissertation, Department of Physics, University of Colorado, 1999.
[62] Veitzer S, Gupta VK. Random self-similar river networks and derivations of generalized Horton laws in terms of statistical simple scaling. Water Resour Res 2000;36(4):1033–48.
[63] Veneziano D, Moglen GE, Bras RL. Multifractal analysis: pitfalls of standard procedures and alternatives. Phys Rev E 1995;52(2):1387–98.
[64] Veneziano D, Moglen GE, Furcolo P, Iacobellis V. Stochastic model of the width function. Water Resour Res 2000;36(4):1143–58.
[65] Waymire E, Williams SC. A cascade decomposition theory with applications to Markov and exchangeable cascades. Trans Am Math Soc 1996;348:585–632.